Fission yeast ortholog of human REEP1-4 is required for autophagosomal enclosure of ER-phagy/nucleophagy cargos

Chen-Xi Zou[1,2], Zhu-Hui Ma[1], Zhao-Qian Pan[1], Dan-Dan Xu[1], Fang Suo[1], Zhao-Di Jiang[1], Li-Lin Du[1,3,*]

[1]National Institute of Biological Sciences, Beijing 102206, China

[2]College of Life Sciences, Beijing Normal University, 100875, Beijing, China

[3]Tsinghua Institute of Multidisciplinary Biomedical Research, Tsinghua University, Beijing 102206, China

*Corresponding authors: dulilin@nibs.ac.cn (L.-L.D.)

Running head: Yep1 is vital for ER-phagy/nucleophagy.

Abstract

Selective macroautophagy of the endoplasmic reticulum (ER) and the nucleus, known as ER-phagy and nucleophagy respectively, are processes whose mechanisms remain inadequately understood. Through an imaging-based screen, we find that fission yeast Yep1, the ortholog of human REEP1-4, is essential for ER-phagy and nucleophagy, but not for bulk autophagy. In the absence of Yep1, the initial phase of ER-phagy and nucleophagy proceeds normally, with the ER-phagy/nucleophagy receptor Epr1 co-assembling with Atg8. However, ER-phagy/nucleophagy cargos fail to reach the vacuole. Instead, nucleus- and cortical-ER-derived membrane structures not enclosed within autophagosomes accumulate in the cytoplasm. This previously unobserved phenotype indicates that ER-phagy/nucleophagy cargo separation from the source compartments is not accompanied by autophagosomal enclosure. We find that the ER-phagy role of Yep1 relies on its abilities to self-interact and shape membranes, and requires its C-terminal amphipathic helices. Moreover, we show that human REEP1-4 and budding yeast Atg40 can functionally substitute for Yep1 in ER-phagy, and Atg40 is a divergent homolog of Yep1 and REEP1-4. Our findings uncover an unexpected mechanism governing the autophagosomal enclosure of ER-phagy/nucleophagy cargos and shed new light on the functions and evolution of REEP family proteins.

Keywords: ER-phagy, nucleophagy, autophagosomal enclosure, REEP family, *Schizosaccharomyces pombe*

Introduction

In eukaryotes, the endoplasmic reticulum (ER) is an intricate membrane organelle composed of interconnected sheet-like structures and tubular networks[1,2]. The formation and maintenance of ER morphology involve two conserved families of integral membrane proteins, the reticulons (RTNs) and the REEP family proteins[3,4]. The ER plays a crucial role in many cellular processes, such as protein folding, lipid synthesis, ion homeostasis, and communication with other organelles[5]. Disturbances of ER functions have been implicated in a wide range of human diseases[6].

Under starvation and ER stress conditions, portions of the ER are turned over through macroautophagy (hereafter autophagy), in a process termed ER-phagy. During ER-phagy, ER membrane fragments are sequestered into autophagosomes, which are double-membrane vesicles that deliver cargos to the lysosome/vacuole for degradation[7,8,9]. In yeasts, the ER mainly consists of the nuclear envelope and the cortical ER[10,11]. Both sub-compartments of the ER can be targeted by ER-phagy. The autophagic sequestration of the nuclear envelope may result in the engulfment of intranuclear components into autophagosomes. Thus, ER-phagy and nucleophagy may occur concurrently[12,13].

The recruitment of the autophagic machinery during ER-phagy and nucleophagy is mediated by specialized autophagy receptors. In recent years, a large number of ER-phagy receptors have been identified, including FAM134B, FAM134A, FAM134C, SEC62, RTN3L, CCPG1, ATL3, TEX264, p62, CALCOCO1, and C53 in mammals[14,15,16,17,18,19,20,21,22,23,24,25], Atg39 and Atg40 in budding yeast[12], and Epr1 in fission yeast[26]. These ER-phagy receptors, which are integral or peripheral ER membrane proteins, all harbor binding motifs for Atg8 family proteins and consequently can mediate the association between the ER and Atg8-decorated autophagic membranes. Some of them solely promote the ER-Atg8 connection during ER-phagy. For example, in the fission yeast *Schizosaccharomyces pombe*, the soluble ER-phagy receptor Epr1, which localizes to the ER through binding integral ER

membrane proteins VAPs, can be rendered dispensable by fusing an Atg8-interacting motif to an integral ER membrane protein Erg11[26]. On the other hand, mammalian FAM134B and budding yeast Atg40, both of which are integral membrane proteins, have roles beyond establishing the ER-Atg8 connection[27,28,29].

In budding yeast and mammalian cells, genetic screenings have uncovered a large number of genes important for ER-phagy[30,31], suggesting that ER-phagy receptors are not the only factors specifically required for ER-phagy. We conduct an imaging-based chemical mutagenesis screen in fission yeast and identify Yep1, the ortholog of human REEP1-4, as a crucial factor in both ER-phagy and nucleophagy. Yep1 is not required for ER-phagy/nucleophagy initiation, but is needed for autophagosomal enclosure of cargo membrane structures that have separated from the source compartments. The ER-phagy function of Yep1 requires not only its first 113 residues that can self-interact and shape ER membrane, but also its C-terminal amphipathic helices, which are dispensable for the membrane-shaping ability. Interestingly, the ER-phagy function of Yep1 can be substituted by human REEP1-4 and budding yeast Atg40. Phylogenetic analysis suggests that Atg40 is a divergent ortholog of Yep1 and REEP1-4. We propose that Yep1 and its equivalents in other eukaryotes play a crucial but previously unanticipated role in ER-phagy and nucleophagy.

Results

Yep1 is required for ER-phagy and nucleophagy

To identify *S. pombe* genes important for ER-phagy, we performed an imaging-based mutant screen (**Figure 1A**). Chemical mutagenesis was applied to a strain in which the copy numbers of 22 general autophagy genes were doubled to reduce the chance of isolating their mutants in the screen. ER-phagy was monitored by examining microscopically the re-localization of the integral ER membrane protein Ost4-GFP to the vacuole upon DTT treatment[32,33,26]. A mutant clone isolated in this screen was subjected to next-generation sequencing-assisted bulk segregant analysis[34], which

indicated that a missense mutation (T17M) in an uncharacterized gene *SPBC30D10.09c* is a candidate causal mutation (**Figure S1A**). For reasons described below, we named this gene *yep1* (for Yop1- and REEP-related protein required for ER-phagy). Yep1 protein belongs to the REEP protein family. This protein family encompasses two subfamilies, both of which are present in most metazoan and fungal species (**Figure 1B**)[35,36,37,38]. There are six REEP family proteins in humans. Among them, REEP1-4 proteins belong to one subfamily and REEP5-6 proteins belong to the other. *S. pombe* has two REEP family proteins, Yep1 and Yop1. Yep1 is the ortholog of human REEP1-4 and Yop1 is the ortholog of human REEP5-6 (**Figure 1B**). Human REEP1-4 are ER-localizing proteins[36,39,40]. Similarly, we found that Yep1 exhibited an ER localization pattern (**Figure S1B**).

Threonine 17 in Yep1 is a conserved residue in REEP1-4 subfamily proteins. Thus, we hypothesized that the T17M mutation may compromise the function of Yep1 and consequently cause an ER-phagy defect. Consistent with this idea, deletion of *yep1* severely diminished the re-localization of Ost4-CFP to the vacuole upon DTT treatment (+DTT) or nitrogen starvation treatment (−N) (**Figure 1C**). *yep1Δ* cells also exhibited a severe defect in the autophagic processing of GFP-tagged integral ER membrane protein Erg11 into free GFP (**Figures 1D and 1E**). Re-introducing Yep1 into *yep1Δ* cells completely rescued the defect. These results indicate that Yep1 is essential for ER-phagy.

As Ost4 and Erg11 localize to both the cortical ER and the nuclear envelope, we also examined the autophagic processing of Rtn1-GFP, which localizes exclusively at the cortical ER, and Ish1-GFP, which is a nuclear envelope protein. The loss of Yep1 abolished DTT- and starvation-induced processing of Rtn1-GFP and Ish1-GFP (**Figures 1F and 1G**), indicating that Yep1 is required for the autophagy of both sub-compartments of the ER.

The observation that the nuclear envelope protein Ish1-GFP is subjected to autophagy suggested to us that the autophagic turnover of nucleoplasmic components,

i.e. nucleophagy, may occur in *S. pombe*. Indeed, under both DTT and starvation treatments, a nucleoplasmic protein Pus1-mECitrine was processed to free mECitrine in an Atg5-dependent manner (**Figures 1H and 1I**). Consistent with the more important role of Epr1 in ER stress-induced ER-phagy than in starvation-induced ER-phagy[26], the loss of Epr1 severely diminished the processing of Pus1-mECitrine in DTT-treated cells but only caused a moderate defect in starved cells. Deletion of *yep1* abolished the processing of Pus1-mECitrine in both DTT- and starvation-treated cells, indicating that Yep1 is essential for nucleophagy.

In contrast to the severe ER-phagy and nucleophagy defects of *yep1Δ* cells, bulk autophagy in *yep1Δ* cells was largely normal as indicated by the processing of CFP-Atg8 (**Figure 1J**). In addition, another readout of bulk autophagy, the processing of fluorescent protein-tagged cytosolic protein Tdh1 (glyceraldehyde-3-phosphate dehydrogenase, GAPDH)[41], was also largely unaffected in *yep1Δ* cells (**Figure S1C**). Consistent with the lack of bulk autophagy defects, transmission electron microscopy (TEM) analysis showed that autophagosome accumulation in the *fsc1Δ* mutant, which is defective in autophagosome-vacuole fusion[42], was not notably affected by the deletion of *yep1* (**Figure S1D**). Inspection of the electron micrographs showed that in *fsc1Δ* cells, there are autophagosomes containing a ring-shaped membrane structure, possibly of the ER/nuclear envelope origin. We call such autophagosomes double-ring structures. The number of double-ring structures per cell was markedly lower in *fsc1Δ yep1Δ* cells than in *fsc1Δ* cells (**Figures S1D and S1E**), suggesting a defect in forming autophagosomes containing ER-phagy and nucleophagy-related cargo membrane structures.

Yep1 acts independently of Epr1 and is not required for the initiation of ER-phagy

The most well-understood type of proteins important for ER-phagy but not bulk autophagy are ER-phagy receptors, whose functions rely on their interactions with Atg8.

We examined whether Yep1 can interact with Atg8 using the Pil1 co-tethering assay[43]. Epr1 but not Yep1 interacted with Atg8 in this assay (**Figure S1F**), indicating that Yep1 is unlikely to be an ER-phagy receptor.

As the proper functioning of the fission yeast ER-phagy receptor Epr1 depends on Ire1, which up-regulates the expression of Epr1 during ER stress[26], we examined the possibility that Yep1 also promotes the expression of Epr1. Immunoblotting analysis showed that ER stress-induced upregulation of the protein level of Epr1 occurred normally in *yep1Δ* cells (**Figure S1G**), ruling out this possibility. Furthermore, even though the role of Epr1 can be bypassed by fusing an artificial AIM to the integral ER membrane protein Erg11[26] (**Figure S1H**), this fusion did not suppress the ER-phagy defect of *yep1Δ* (**Figure S1I**), indicating that the main role of Yep1 is not promoting the function of Epr1. Consistent with this idea, increasing the level of Epr1 did not suppress *yep1Δ* (**Figure S1I**), and increasing the level of Yep1 did not suppress *epr1Δ* (**Figure S1H**). Together, these results suggest that Yep1 and Epr1 play different roles in ER-phagy.

Next, we monitored the localization of Epr1 and Atg8 during ER-phagy. In both wild-type and *yep1Δ* cells, Epr1 and Atg8 co-localized at punctate structures shortly after ER-phagy induction by DTT or starvation treatment (**Figure S2A**), indicating that Yep1 is not essential for the initial stage of ER-phagy during which Epr1 mediates a connection between the ER and Atg8-decorated autophagic membranes.

Yep1 is required for the autophagosomal enclosure of ER-phagy and nucleophagy cargos

In our analysis of the nucleophagy defect of *yep1Δ*, we noticed that two markers of the cargo compartment, the inner nuclear membrane protein Bqt4 and the nucleoplasmic protein Pus1, formed cytoplasmic puncta in *yep1Δ* cells after ER-phagy induction (**Figures 2A and 2B**). No Bqt4 or Pus1 puncta were observed in *atg5Δ* cells

and *yep1Δ atg5Δ* cells, suggesting that these puncta are autophagy-related structures. Under starvation treatment, no Bqt4 or Pus1 puncta were observed in wild-type cells. Under DTT treatment, a smaller number of Bqt4 or Pus1 puncta were observed in wild-type cells, possibly because DTT treatment causes a mild accumulation of autophagosomes in the cytoplasm (see below). We examined whether Bqt4 puncta and Pus1 puncta in *yep1Δ* cells co-localize and found that, Pus1 puncta almost always overlapped with Bqt4 puncta and a great majority (> 80%) of Bqt4 puncta overlapped with Pus1 puncta (**Figures 2C and S2B**). Thus, the nucleophagy defect of *yep1Δ* is accompanied by the accumulation of nucleus-derived membrane structures containing inner nuclear membrane components and nucleoplasmic components.

To better understand the nature of the structures represented by cytoplasmic puncta of Bqt4 and Pus1, we performed TEM analysis. This analysis showed that ring-shaped membrane structures accumulated in the cytoplasm of *yep1Δ* cells but not *yep1Δ atg5Δ* cells (**Figures 2D, S2C and S2D**). These structures differ in location from the ring-shaped autophagosomes accumulated in the *fsc1Δ* cells (**Figure S1D**). Autophagosomes accumulated in the *fsc1Δ* cells are almost always juxtaposed to vacuoles. In contrast, ring-shaped membrane structures in the cytoplasm of *yep1Δ* cells were never observed juxtaposed to vacuoles. The shape and size of these structures are similar to those of the inner rings in the double-ring structures observed in the *fsc1Δ* cells (**Figure S2E**). Thus, we proposed that these structures are ER-phagy/nucleophagy cargos that had separated from the source compartments but were not enclosed within autophagosomes, and they include structures represented by the Bqt4 and Pus1 puncta. In DTT-treated but not starvation-treated wild-type cells, autophagosomes juxtaposed to vacuoles can be observed (**Figure S2C**). They likely include structures corresponding to the Bqt4 and Pus1 puncta observed in wild-type cells by fluorescence microscopy.

To further examine the nature of the ring-shaped membrane structures accumulated in the cytoplasm of *yep1Δ* cells, we fused an genetically encoded EM tag,

MTn, to the integral ER membrane protein Ost4 and examined its distribution in *yep1Δ* cells using a recently developed EM technology[44]. MTn-generated gold nanoparticles were observed not only on the nuclear envelope and the cortical ER, but also on ring-shaped cytoplasmic membrane structures resembling the ring-shaped structures observed in the TEM analysis (**Figure 2E**), confirming that nucleus- and/or cortical-ER-derived structures without surrounding autophagic membranes accumulate in the cytoplasm of *yep1Δ* cells.

To obtain more corroborating evidence on the accumulation of ER-phagy/nucleophagy cargos in *yep1Δ* cells, we employed the degron protection assay[45]. In this assay, an auxin-inducible degron (AID) tag is fused to a protein so that the protein is degraded when exposed to the cytosol but not when residing inside a membrane compartment. We used the cytosolic protein Pyk1, a bulk autophagy cargo, to verify whether a protein enclosed within the autophagosome is resistant to AID-mediated degradation. In untreated cells, Pyk1-AID-mECitrine was completely degraded upon the addition of the auxin analog 5-adamantyl-IAA (Ad-IAA)[46] (**Figure S2F**). When autophagy was induced by nitrogen starvation, Pyk1-AID-mECitrine signal in small round-shaped structures, which are vacuoles labelled by the vacuole lumen marker Cpy1-mCherry, persisted in wild-type cells after the addition of Ad-IAA. Similarly, persisting Pyk1-AID-mECitrine signal in vacuoles was observed in nitrogen-starved *yep1Δ* cells, confirming that bulk autophagy is largely normal in *yep1Δ* cells. In *fsc1Δ* cells, which are defective in autophagosome-vacuole fusion, persisting Pyk1-AID-mECitrine signal in structures not overlapping with vacuoles was observed after the addition of Ad-IAA. These structures are presumably autophagosomes, suggesting that AID-mediated degradation does not happen to proteins enclosed within autophagosomes. For our analysis of ER-phagy/nucleophagy cargos accumulated in *yep1Δ* cells, we chose Epr1 as the degradation target as it is a peripheral membrane protein facing the cytosol and is concentrated at the sites of ER-phagy/nucleophagy. As expected, in untreated wild-type or *yep1Δ* cells, signals of Epr1-AID-mECitrine

completely disappeared after the addition of Ad-IAA (**Figure S2G**). In contrast, in wild-type cells starved for 6 h, Epr1-AID-mECitrine re-localized to the vacuole lumen, and the vacuolar signal persisted after the addition of Ad-IAA. In *yep1Δ* cells, Epr1-AID-mECitrine formed cytoplasmic puncta, some of which co-localized with Pus1 cytoplasmic puncta. Upon the addition of Ad-IAA, Epr1-AID-mECitrine puncta completely disappeared (**Figure S2G**), indicating that in *yep1Δ* cells, the outer surface of nucleus-derived membrane structures accumulated in the cytoplasm is exposed to the cytosol.

To determine whether cortical-ER-derived membrane structures not enclosed within autophagosomes also accumulated in *yep1Δ* cells, we applied the degron protection assay to the integral ER membrane protein Rtn1, which localizes to the cortical ER but not the nuclear envelope (**Figure S2H**). Rtn1-AID-mECitrine signal in untreated wild-type and *yep1Δ* cells disappeared upon the addition of Ad-IAA. In starvation treated wild-type cells, Rtn1-AID-mECitrine partially re-localized to the vacuole lumen and the vacuole-localized signal persisted upon the addition of Ad-IAA. In starvation treated *yep1Δ* cells, Rtn1-AID-mECitrine formed cytoplasmic puncta, which disappeared after the addition of Ad-IAA (**Figure S2H**), suggesting that like the situation of the nucleophagy cargo, the cortical-ER-phagy cargo also undergoes separation from the source membrane compartment but fails to be enclosed within autophagosomes in *yep1Δ* cells. Taken together, the above results demonstrate that Yep1 is required for the autophagosomal enclosure of cargos during ER-phagy and nucleophagy but not the formation of cargo membrane structures and their separation from the source compartments.

Yep1 possesses the ability to shape the ER membrane

In fission yeast, three ER-shaping proteins, the REEP family protein Yop1, the reticulon family protein Rtn1, and the TMEM33 family protein Tts1, localize to tubular

ER and act in a partially redundant manner to maintain tubular ER[47]. We observed that Yep1 exhibited co-localization with Rtn1, Yop1, and Tts1 (**Figures 3A and S3A**), suggesting that Yep1 may share similar functions with these proteins.

In the absence of Rtn1, Yop1, and Tts1, the cortical ER becomes less reticulate and more sheet-like, with the frequent appearance of large holes in images of the top or bottom plane of the cells and extended gaps in images of the mid-plane of the cells[47]. We found that this alteration of ER morphology can be reversed to a large extent by either introducing back Rtn1 or increasing the expression level of Yep1 (**Figures 3B and S3B**). Thus, Yep1, when overexpressed, can fulfill the function of maintaining tubular ER independently of Rtn1, Yop1, and Tts1.

The ER structure aberration caused by the loss of Rtn1, Yop1, and Tts1 also leads indirectly to a severe septum positioning defect, manifested as long-axis septum, multiple septa, and tilted septum[47]. This phenotype is easier to score than the ER morphology phenotype and can reveal the weak phenotypes of single deletion mutants lacking Rtn1, Yop1, or Tts1 (**Figure 3C**). We observed that *yep1Δ* caused a noticeable but even weaker septum positioning defect than *rtn1Δ*, *yop1Δ*, or *tts1Δ*. Combined *yep1Δ* with the double and triple deletion of *rtn1*, *yop1*, and *tts1* invariably resulted in a more severe phenotype (**Figures 3C**). The most pronounced phenotypic enhancement was observed when *yep1Δ* was combined with the *rtn1Δ tts1Δ* double deletion. The defect of *rtn1Δ tts1Δ yep1Δ* can be rescued to the level of *rtn1Δ tts1Δ* by re-introducing Yep1 (**Figure S3C**). Moreover, increasing the expression level of Yep1 ameliorated the septum positioning defect of *rtn1Δ yop1Δ tts1Δ* (**Figure S3D**). These results demonstrate that Yep1 shares the membrane-shaping ability of Rtn1, Yop1, and Tts1 and contributes to the maintenance of normal ER structure.

We assessed whether Rtn1, Yop1, and Tts1 function in ER-phagy. DTT and starvation-induced processing of Erg11-GFP was only slightly diminished in the *rtn1Δ yop1Δ tts1Δ* triple deletion mutant (**Figure 3D**), suggesting that ER-phagy still occurs in the absence of these three proteins. In addition, overexpression of Rtn1, Yop1, or

Tts1 did not alleviate the severe ER-phagy defect of *yep1Δ* (**Figure 3E**). Thus, Rtn1, Yop1, and Tts1 cannot substitute for the essential role of Yep1 in ER-phagy.

Yep1 self-interaction is important for its membrane-shaping ability and ER-phagy function

Several ER-shaping proteins, including Yop1, are known to self-interact[3,4,48,49,50]. It has been proposed that the formation of arc-shaped homo-oligomer is one mechanism responsible for generating the tubular membrane shape[51]. Using the co-immunoprecipitation assay, we found that Yep1 can self-interact (**Figure 4A**). Bimolecular fluorescence complementation (BiFC) confirmed the self-interaction of Yep1 and suggested that Yep1 undergoes self-interaction on the ER membrane (**Figure S4A**).

We used AlphaFold-Multimer to predict the structures of Yep1 homo-oligomers[52] (**Figure 4B and S4B**). Regardless of the number of Yep1 sequences (from two to eight) in the input, AlphaFold-Multimer only predicted one type of oligomeric structure—the structure of the Yep1 dimer, indicating that the dimer is the preferred oligomerization state of Yep1. In the predicted structure of the Yep1 dimer (**Figure 4C**), within each Yep1 molecule, there are three long α-helices in the N-terminal region. They largely encompass the three transmembrane segments predicted by TOPCONS (**Figures 4D and S4C**). The C-terminal cytoplasmic region contains two short α-helices, two long α-helices, and a disordered tail[53] (**Figures 4D and S4C**). Inter-molecular contacts mainly involve the first two transmembrane helices (TMHs). The two short C-terminal helices (amino acids 98-113) also contribute to the dimer interface by engaging the N-terminal helices of the other molecule (**Figure 4C and S4D**).

Consistent with the predicted structure of the Yep1 dimer, Yep1(1-97) failed to exhibit self-interaction in the co-immunoprecipitation analysis (**Figure 4E**), whereas Yep1(1-113) was able to self-interact (**Figure 4F**). The septum positioning defect of

rtn1Δ tts1Δ yep1Δ was rescued to the level of *rtn1Δ tts1Δ* by the expression of Yep1(1-113), but not Yep1(1-97) (**Figure 4G)**, suggesting that the membrane-shaping ability of Yep1 depends on its self-interaction. Internal deletion of residues 98-113 abolished the abilities of Yep1 to self-interact and to rescue the septum positioning defect of *rtn1Δ tts1Δ yep1Δ* (**Figures 4H and 4G**). Moreover, Yep1 lacking residues 98-113 can no longer support ER-phagy (**Figure 4I**). Together, these results suggest that Yep1 self-interaction is important for its membrane-shaping ability and imply that the membrane-shaping ability is important for its role in ER-phagy.

Amphipathic helices of Yep1 are essential for its ER-phagy function

Even though Yep1(1-113) can self-interact and possesses the membrane-shaping ability, it cannot support ER-phagy in *yep1Δ* cells (**Figure 5A**). In contrast, Yep1(1-131) and Yep1(1-150), which contained one and two additional C-terminal long helices, respectively, can support ER-phagy. Internal deletion of both but not either one of these two helices abolished the ER-phagy function of Yep1, suggesting that these two long helices play redundant roles for the ER-phagy function of Yep1 (**Figure 5B**). Consistent with the results obtained on Yep1(1-113), the internal deletion mutant Yep1Δ(114-150), which lacks both long helices, and Yep1(1-150) can self-interact and can rescue *rtn1Δ tts1Δ yep1Δ* to the same extent as full-length Yep1 (**Figures S5A, S5B, S5C, and S5D**).

HeliQuest analyses of the C-terminal helices and visual inspection of the AlphaFold-predicted structure indicated that these two long helices are amphipathic helices (APHs), whereas the two upstream short helices do not exhibit obvious amphipathicity[54] (**Figures 5C, S5E, and S5F**). To examine whether the amphipathic nature of these two APHs is functionally important, we substituted three hydrophobic amino acids with aspartates in each APH to disrupt their hydrophobic face[55,56]. Mutating either APH did not abolish the ER-phagy function of Yep1, whereas mutating

both APHs rendered the protein nonfunctional in ER-phagy (**Figures 5D and S5G**). Together, these results demonstrate that these APHs are redundantly essential for the ER-phagy function of Yep1.

REEP1-4 subfamily proteins and Atg40 share the same ER-phagy function with Yep1

To understand whether the structural features of Yep1 are conserved in its homologs, we applied the same analyses, including the inspection of AlphaFold predicted structures, TOPCONS prediction of membrane topology, and HeliQuest analysis of APHs, to several other representative REEP family proteins (**Figures 6A and 6B**). Consistent with a previous report[50], our analyses showed that REEP1-4 subfamily proteins have three TMHs, whereas REEP5-6 subfamily proteins have four TMHs. They all contain APHs in the C-terminal cytoplasmic region. REEP5-6 subfamily proteins also possess APHs in the N-terminal cytoplasmic region.

In *S. pombe,* as our data show (**Figure 3E**), the REEP5-6 subfamily member Yop1 cannot substitute for the ER-phagy function of the REEP1-4 subfamily member Yep1. We examined whether exogenously expressing human REEP family proteins can suppress the ER-phagy defect of *yep1Δ*. Remarkably, REEP1 and REEP3 fully suppressed *yep1Δ*, and REEP2 and REEP4 exhibited partial suppression (**Figure 6C**). In contrast, REEP5 and REEP6 showed no suppression (**Figure 6C**). These results suggest that REEP1-4 subfamily proteins but not REEP5-6 subfamily proteins share a conserved ER-phagy function with *S. pombe* Yep1.

Even though *S. cerevisiae* does not have an obvious REEP1-4 subfamily member, a known ER-phagy receptor in *S. cerevisiae*, Atg40, resembles REEP1-4 subfamily proteins in the number and topology of its TMHs[29]. Our analysis showed that it also possesses APHs downstream of its three TMHs (**Figures 6A, 6B, and S6A**). To understand the relationship between Atg40 and REEP1-4 subfamily proteins, we

surveyed the species distribution of Atg40 homologs and REEP1-4 subfamily proteins in the *Ascomycota* phylum (**Figure 6D**). PSI-BLAST-detectable sequence homologs of Atg40 (hereafter referred to as Atg40 proteins) were only found in budding yeast species belonging to the *Saccharomycetaceae* family. Interestingly, these species all lack a REEP1-4 subfamily protein. In contrast, *Ascomycota* species outside of the *Saccharomycetaceae* family all have at least one REEP1-4 subfamily protein. Remarkably, within the subphylum *Saccharomycotina* (budding yeasts), species not belonging to the *Saccharomycetaceae* family all possess one REEP1-4 subfamily protein harboring a C-terminal AIM, resembling the situation in Atg40 (**Figures 6D and S6B**). These observations suggest that Atg40 proteins are divergent homologs of REEP1-4 subfamily proteins. Supporting this idea, a phylogenetic analysis showed that Atg40 proteins and *Ascomycota* REEP1-4 subfamily proteins fall into the same clade, and *Ascomycota* REEP5-6 subfamily proteins fall into a sister clade (**Figure S6C**).

Consistent with the results of the phylogenetic analysis, ectopic expression of Atg40 in *S. pombe* rescued the ER-phagy defect of *yep1Δ* (**Figure 6E**). In contrast, the other *S. cerevisiae* ER-phagy receptor, Atg39, failed to rescue *yep1Δ*. The ability of Atg40 to rescue *yep1Δ* is independent of its AIM (**Figure 6E**). Interestingly, ectopic expression of Atg40 in *S. pombe* can also rescue the ER-phagy defect of *epr1Δ*, and this rescue requires its AIM (**Figure S6D**). Moreover, Atg40 can even rescue the ER-phagy defect of the *yep1Δ epr1Δ* double mutant (**Figure S6E**), suggesting that Atg40 fulfills the combined roles of Yep1 and Epr1 in ER-phagy.

We examined the role of the APHs in Atg40 by truncation analysis. Atg40(1-193), which lacks the C-terminal disordered tail, was still able to rescue the ER-phagy defect of *yep1Δ* (**Figures 6F and 6G**). In contrast, Atg40(1-153), which lacks the two C-terminal APHs, failed to support ER-phagy in *yep1Δ* cells (**Figures 6F, and 6G**). To address the question why REEP1-4 subfamily proteins and Atg40 but not REEP5-6 subfamily proteins can substitute for Yep1, we replaced the C-terminal region of Yep1 with a C-terminal APH-encompassing segment of *S. cerevisiae* Atg40 or *S. pombe*

Yop1. The ER-phagy defect of *yep1Δ* can be suppressed to a similar extent by the two mosaic proteins (**Figures S6F and 6H**), indicating that the C-terminal APHs of REEP5-6 subfamily proteins are capable of supporting ER-phagy. One possibility is that the extra TMH and/or the cytoplasmic tail in the N-termini of REEP5-6 subfamily proteins are incompatible with ER-phagy. Supporting this possibility, we found that adding the N-terminal region of Yop1 upstream of its second TMH or only the first TMH of Yop1 to the N-terminus of Yep1 disrupted the ER-phagy function of Yep1 (**Figures S6F and S6G**). However, the presence of the extra N-terminal sequence may not be the only reason why REEP5-6 subfamily proteins cannot support ER-phagy, as removing the N-terminal region of Yop1 upstream of its second TMH did not render it capable of substituting for Yep1 (**Figures S6F and S6H**).

Discussion

In this study, through an imaging-based chemical mutagenesis screen, we identify Yep1 as an essential factor for ER-phagy. Our follow-up investigation reveals that Yep1 is crucial for ER-phagy/nucleophagy under ER-stress and starvation conditions, but is dispensable for bulk autophagy. In the absence of Yep1, the recruitment of the autophagic machinery at the early phase of ER-phagy/nucleophagy occurs normally, but ER- and nucleus-derived structures without surrounding autophagic membranes accumulate in the cytoplasm, indicating that Yep1 plays a critical role in the autophagosomal enclosure of cargos during ER-phagy/nucleophagy (**Figure 7**). This is a surprising finding, as no previously known ER-phagy/nucleophagy factors have been implicated in such a role.

The best understood ER-phagy factors are ER-phagy receptors, which mediate the recruitment of the autophagic machinery. Several ER-phagy receptors have been shown to have additional functions. For example, FAM134 family proteins and RTN3L promote the fragmentation of ER membranes[15,16,18,27,28], and Atg40 bends ER membranes to facilitate ER packaging into autophagosomes[29]. Non-receptor ER-phagy factors can be classified into two types based on their functions. The first type promotes ER-phagy through regulating ER-phagy receptors. Examples of this type include Ire1 that upregulates the protein level of Epr1[26], CK2 that enhances the Atg8-binding affinity of TEX264[57], and CAMK2B that promotes FAM134B oligomerization[28]. The second type, mainly studied in *S. cerevisiae*, acts in concert with ER-phagy receptors to promote the formation of ER-phagy sites or the packaging of ER membranes into autophagosomes. This type of factors includes Lnp1[58], the Lst1-Sec23 complex[59], Vps13[30], and a group of proteins regulating actin assembly at sites of contact between the cortical ER and endocytic pits[60]. The loss of any essential ER-phagy factors invariably results in the failure to form autophagosomes containing ER membranes. However, it has not been reported before that ER membrane-derived cytoplasmic structures without surrounding autophagic membranes accumulate in an ER-phagy

mutant. Thus, our findings reveal an unexpected mechanism ensuring the successful autophagosomal enclosure of cargos during ER-phagy, and indicate that ER membrane fragmentation and autophagosomal enclosure of ER fragments can be uncoupled during ER-phagy.

Compared to ER-phagy, nucleophagy is more poorly understood. It is unclear to what extent nucleophagy shares the same underlying mechanisms with ER-phagy. *S. cerevisiae* Atg39 is the only known autophagy receptor with a dedicated role in nucleophagy[14]. Atg39 has non-receptor functions in linking the inner and outer nuclear membranes and in deforming the nuclear envelope to generate nucleus-derived double-membrane vesicles enclosed in autophagosomes[13]. No non-receptor factors required for nucleophagy have been reported. Our findings here show that in *S. pombe*, Epr1 serves as an autophagy receptor for both nucleophagy and ER-phagy, and Yep1 is required for autophagosomal enclosure of cargos during both nucleophagy and ER-phagy, suggesting that these two processes share a common set of factors.

The exact role of Yep1 in ER-phagy/nucleophagy remains unclear. Here, we discuss two possibilities based on the requirement of its membrane-shaping ability: Yep1 may remodel cargo membranes, or it may help shaping autophagic membranes. These two possibilities are not mutually exclusive.

In the first possibility, as an integral ER membrane protein, Yep1 may exert its function on the ER/nuclear envelope. We envision that Yep1 may contribute to but is not absolutely necessary for ER fragmentation and the generation of nucleus-derived vesicles during ER-phagy/nucleophagy. This is a role similar to the non-receptor role proposed for RTN3L and FAM134B. Loss of Yep1 may delay but not completely prevent ER/nuclear envelope membrane scission. This delay may disrupt the coordination between membrane scission and autophagosomal enclosure and results in the formation of ER/nucleus-derived cytoplasmic structures not enclosed in autophagosomes. Alternatively, Yep1 may not participate in the fragmentation of cargos but rather facilitate autophagosomal enclosure by bending cargo membranes in

a certain way to allow a better fit of the cargo membranes within the surrounding autophagic membranes. This is a role analogous to the one proposed for *S. cerevisiae* Atg40.

In the second possibility, some Yep1 molecules may re-localize from the ER to the isolation membrane and play a role in shaping the isolation membrane. We speculate that this re-localization may take the route of COPII vesicles, which have been shown to transport an integral ER membrane protein to the autophagic membranes[61]. If Yep1 functions on the isolation membrane, it begs the question: why is Yep1 essential for ER-phagy/nucleophagy but dispensable for bulk autophagy? We speculate that one possible explanation is that different types of autophagy may utilize different membrane sources for the isolation membrane. As a result, the isolation membrane for ER-phagy/nucleophagy may have a protein composition different from the isolation membrane for bulk autophagy, and Yep1 is not important for bulk autophagy because there are other factors playing a similar function on the isolation membrane for bulk autophagy. Another possibility is that the size and shape of ER-phagy/nucleophagy cargos impose a special requirement for the shape of the isolation membrane, and Yep1 is needed to meet this requirement.

During the preparing of this manuscript, a preprint by Wang et al. reports the identification of Yep1 (called Rop1 in that study) as an autophagy factor[62]. They show that Yep1 localizes to the isolation membrane, supporting the second possibility discussed above. There are several discrepancies between the two studies. Yep1 is found to be largely dispensable for bulk autophagy in our study but shown to be important for bulk autophagy by Wang et al. In addition, we show that Atg40 can substitute for the role of Yep1 in ER-phagy, while Wang et al. shows that Atg40 fails to suppress the sensitivity of *yep1Δ* to ER stress. The exact reasons of these discrepancies are unclear but may be related to differences in strain backgrounds and assaying conditions.

Based on the phylogenetic analysis results shown here (**Figure 1B**) and elsewhere[35,36,37,38], both the REEP1-4 subfamily and the REEP5-6 subfamily exist in the common ancestor of animals and fungi. The findings that human REEP1-4 but not REEP5-6 can substitute for the ER-phagy function of Yep1 indicate that the REEP1-4 subfamily may have an ancestral role in ER-phagy. Our analyses of the evolutionary relationships of REEP family proteins in the *Ascomycota* phylum (**Figures 6D, S6B, and S6C**) suggest that in the *Saccharomycotina* subphylum (budding yeasts), the ER-phagy role of the REEP1-4 subfamily proteins is further enhanced by the acquisition of a C-terminal AIM so that they can also act as ER-phagy receptors. For reasons unclear, substantial sequence divergence happened to the REEP1-4 subfamily proteins in the common ancestor of the *Saccharomycetaceae* family, giving rise to the Atg40 proteins. Further studies will be needed to understand to what extent REEP1-4 subfamily proteins in different species share common ER-phagy functions and mechanisms.

Methods

Strain and plasmid construction

Fission yeast strains used in this study are listed in Table S1, and plasmids used in this study are listed in Table S2. The genetic methods for strain construction and composition of media are as previously described[63]. Deletion strains were generated by PCR-based gene targeting. The strain containing one additional copy of each of 22 core autophagy genes (*atg2*, *atg3*, *atg4*, *atg5*, *atg6*, *atg7*, *atg8*, *atg9*, *atg10*, *atg11*, *atg12*, *atg13*, *atg14*, *atg16*, *atg17*, *atg18a*, *atg18b*, *atg18c*, *atg101*, *vps34*, *vps15*, and *ctl1*) was constructed using the CRISPR-Cas9 system[64]. The plasmids expressing proteins fused with different N-terminal or C-terminal tags (GFP, CFP, mECtrine, mCherry, mTurquoise2) under exogenous promoters (*P41nmt1*, *Pnmt1*, or *Padh1*) were constructed utilizing modified pDUAL vectors[65] or modified SIV vectors[66]. The plasmids expressing Erg11-AIM^{art} were based on modified SIV vectors. AIM^{art} corresponds to 3×EEEWEEL[67].

Screening for mutants defective in ER-phagy

Log phase cells were harvested and resuspended in 0.3 ml of TM buffer (50 mM Tris-maleate). Mutagenesis was induced by adding 0.1 ml of 2 mg/ml N-methyl-N′-nitro-N-nitrosoguanidine (MNNG) to the cell suspension and incubating at room temperature for 60 minutes. The mutagenized cells were then plated on the EMM medium and incubated at 30 °C for 4 days. Small and medium-sized colonies were selected, transferred to 96-well deep-well plates, grown for 24 hours in EMM liquid medium at 30 °C, and treated with 10 mM DTT for 12 hours to induce ER-phagy. A high-content imaging system (Opera LX, PerkinElmer) was used for observing the subcellular localization of Ost4-GFP. Candidate mutants defective in vacuolar re-localization of Ost4-GFP were further evaluated using a DeltaVision PersonalDV system (Applied Precision). Strains whose phenotypes were confirmed by reexamination were backcrossed, and the backcrossed progeny were analyzed via next-generation

sequencing-assisted bulk segregant analysis[68]. For each backcross, mutations enriched in ER-phagy defective progeny were considered as the candidate phenotype-causing mutations.

Fluorescence microscopy

Live-cell imaging was performed using a DeltaVision PersonalDV system (Applied Precision) and a Dragonfly high-speed confocal microscope system (Andor Technology). The DeltaVision system was equipped with a 100×, 1.4-NA objective, an mCherry/YFP/CFP filter set, and a Photometrics EMCCD camera. The Dragonfly system was equipped with a 100×, 1.4-NA objective, an mCherry/YFP/CFP filter set, an mCherry/GFP filter set, and a Sona sCMOS camera. Image analysis was conducted using the SoftWoRx software and Fiji (ImageJ). Co-localization analysis using PCC was performed as previously described (Zhao ,yu).

Immunoblotting-based protein processing assay

5.0 OD_{600} units of cells expressing a GFP-tagged protein (Erg11, Ish1, or Rtn1), an mECtirine-tagged protein (Pus1), or a CFP-tagged protein (Atg8 or Tdh1) were harvested. The cells were mixed with 300 μl of 20% trichloroacetic acid (TCA) and lysed by beating with 0.5-mm-diameter glass beads using a FastPrep instrument at a speed of 6.5 m/s for three cycles of 20 seconds each. The cell lysate was centrifuged and the pellet was resuspended in HU buffer (150 mM Tris·HCl, 6% SDS, 6 M urea, 10% 2-mercaptoethanol, 0.002% bromophenol blue, pH 6.8) and incubated at 42 °C for 20 min. The samples were then separated by 10% SDS-PAGE and immunoblotted with antibodies. The antibodies used for immunoblotting were anti-GFP mouse monoclonal antibody (1:3,000 dilution, Roche, 11814460001) and anti-mCherry mouse monoclonal antibody (1:3,000 dilution, Huaxingbio, HX1810).

Electron microscopy

For regular transmission electron microscopy (TEM) analysis, 50 OD_{600} units of cells were harvested after being starved for 12 hours or treated with 10 mM DTT for 12 h. Cells were fixed with 1% glutaraldehyde and 4% KMnO4 and dehydrated through a graded ethanol series. The samples were then embedded in Spurr's resin[69]. Thin sections were examined using an FEI Tecnai G2 Spirit electron microscope equipped with a Gatan 895 4k×4k CCD camera. The diameters of the ring-shaped structures were determined using the method previously used for measuring the sizes of autophagosomes or autophagic bodies[41,70]. P-values were calculated using Welch's t-test. For electron microscopy analysis employing the genetically encoded EM tag MTn, samples were prepared as previously described[44]. Briefly, 20 OD600 units of cells expressing Ost4-MTn were harvested after treatment with 10 mM DTT for 12 h. Cells were incubated with 3 mM dithiodipropionic acid (DTDPA) in 0.1 M PIPES at 4°C for 30 min and then treated with 0.5 mg/ml zymolyase 20T and 50 mM DTT in PBS buffer for 10 minutes to remove the cell wall. The zymolyase-treated cells were permeabilized with 0.05% Triton X-100 for 5 min, and processed for gold nanoparticle synthesis. Cells were mixed with 60 mM 2-mercaptoethanol, 0.5 mM $HAuCl_4$, 50 mM diphenylethylenediamine (DPEN), and 10 μM $NaBH_4$, and subjected to standard high-pressure freezing/freeze-substitution fixation. After resin infiltration, embedding, polymerization, and thin sectioning, the samples were used for EM imaging as described above.

Pil1 co-tethering assay

To investigate the Atg8-interacting ability, Yep1 and Epr1 were fused to GFP as the prey, and Atg8 was fused to Pil1-mCherry as the bait[43]. Log-phase cells co-expressing both proteins were then analyzed by fluorescence microscopy.

Protein depletion using the auxin-inducible degron (AID)

Cells cultured in EMM liquid media at 30 °C were used. Prior to observation, cells in EMM liquid media were treated with 1 μM 5-adamantyl-IAA for 1.5 hours at 30 °C[46].

Immunoprecipitation

100 OD_{600} units of log-phase cells were harvested. Cells were mixed with 150 μl of lysis buffer (50 mM HEPES-NaOH pH 7.5, 150 mM NaCl, 1 mM EDTA, 1 mM DTT, 1 mM PMSF, 0.05% NP-40, 10% glycerol, 1×Roche protease inhibitor cocktail) and were lysed by beating with 0.5-mm-diameter glass beads using a FastPrep instrument at a speed of 6.5 m/s for three cycles of 20 seconds each. The lysate was incubated with GFP-Trap agarose beads at 4°C for 3 hours. The beads were washed twice and proteins were eluted by boiling in SDS-PAGE loading buffer. Samples were separated by 10% SDS-PAGE and analyzed by immunoblotting using anti-GFP and anti-mCherry antibodies described above.

Bi-fluorescence complementation (BiFC) assays

To investigate the self-interaction of Yep1, the N-terminal Venus fragment (VN173) and the C-terminal Venus fragment (VC155) were fused to Yep1, respectively[71]. Log-phase cells co-expressing the VN173 fusing protein and the VC155 fusing protein were analyzed by fluorescence microscopy.

Phylogenetic analysis

Protein sequences were aligned using the L-INS-i iterative refinement algorithm of MAFFT on the online MAFFT server (https://mafft.cbrc.jp/alignment/server/)[72]. The maximum likelihood trees were calculated using IQ-TREE (version 2.1.3) for Mac OS X[73]. Trees were rooted by midpoint rooting and visualized using FigTree (version 1.4.4) (http://tree.bio.ed.ac.uk/software/figtree/).

Prediction of protein structures, transmembrane topology, and amphipathic helices

The structures of the Yep1 monomer and oligomers were predicted using AlphaFold-Multimer (version 2.2.0) with default parameters[52]. The structure with the highest confidence score among the predicted output was selected for further analysis. The predicted structures were visualized using the Mol* Viewer (version 2.5.0). The transmembrane topology was predicted using the TOPCONS web server (https://topcons.cbr.su.se/pred/)[53]. The amphipathic nature of helices was analyzed using the HeliQuest web server (https://heliquest.ipmc.cnrs.fr/cgi-bin/ComputParams.py)[54].

Acknowledgements

We are grateful to Yin Liu and He-Xia Luo of the NIBS electron microscopy facility for helps in EM analysis. This work was supported by grants from the Ministry of Science and Technology of the People's Republic of China and the Beijing municipal government.

Author contributions

Conceptualization: C.-X.Z. and L.-L.D.; Investigation: C.-X.Z., Z.-H.M., Z.-Q.P., D.-D.X., F.S., Z.-D.J., and L.-L.D.; Writing – original draft: C.-X.Z. and L.-L.D.; Writing – review and editing: C.-X.Z. and L.-L.D.

Competing interests

The authors declare no competing interests.

Materials & Correspondence

Correspondence and requests for materials should be addressed to L.-L.D.

References

1. Structural organization of the endoplasmic reticulum. *EMBO reports* **3**, 944–950 (2002).
2. Chen, S., Novick, P. & Ferro-Novick, S. ER structure and function. *Current Opinion in Cell Biology* **25**, 428–433 (2013).
3. Voeltz, G. K., Prinz, W. A., Shibata, Y., Rist, J. M. & Rapoport, T. A. A class of membrane proteins shaping the tubular endoplasmic reticulum. *Cell* **124**, 573–586 (2006).
4. Hu, J. *et al.* Membrane Proteins of the Endoplasmic Reticulum Induce High-Curvature Tubules. *Science* **319**, 1247–1250 (2008).
5. Schwarz, D. S. & Blower, M. D. The endoplasmic reticulum: structure, function and response to cellular signaling. *Cell. Mol. Life Sci.* **73**, 79–94 (2016).
6. Hebert, D. N. & Molinari, M. In and Out of the ER: Protein Folding, Quality Control, Degradation, and Related Human Diseases. *Physiological Reviews* **87**, 1377–1408 (2007).
7. Grumati, P., Dikic, I. & Stolz, A. ER-phagy at a glance. *Journal of Cell Science* **131**, jcs217364 (2018).
8. Molinari, M. ER-phagy responses in yeast, plants, and mammalian cells and their crosstalk with UPR and ERAD. *Developmental Cell* **56**, 949–966 (2021).
9. Mochida, K. & Nakatogawa, H. ER-phagy: selective autophagy of the endoplasmic reticulum. *EMBO reports* **23**, e55192 (2022).
10. Preuss, D. *et al.* Structure of the yeast endoplasmic reticulum: Localization of ER proteins using immunofluorescence and immunoelectron microscopy. *Yeast* **7**, 891–911 (1991).
11. West, M., Zurek, N., Hoenger, A. & Voeltz, G. K. A 3D analysis of yeast ER structure reveals how ER domains are organized by membrane curvature. *Journal of Cell Biology* **193**, 333–346 (2011).
12. Mochida, K. *et al.* Receptor-mediated selective autophagy degrades the endoplasmic reticulum and the nucleus. *Nature* **522**, 359–362 (2015).
13. Mochida, K. *et al.* Atg39 links and deforms the outer and inner nuclear membranes in selective autophagy of the nucleus. *Journal of Cell Biology* **221**, e202103178 (2022).
14. Khaminets, A. *et al.* Regulation of endoplasmic reticulum turnover by selective autophagy. *Nature* **522**, 354–358 (2015).
15. Reggio, A. *et al.* Role of FAM134 paralogues in endoplasmic reticulum remodeling, ER-phagy, and Collagen quality control. *EMBO Reports* **22**, (2021).
16. Kumar, D. *et al.* RTN4B interacting protein FAM134C promotes ER membrane curvature and has a functional role in autophagy. *MBoC* **32**, 1158–1170 (2021).
17. Fumagalli, F. *et al.* Translocon component Sec62 acts in endoplasmic reticulum turnover during stress recovery. *Nature Cell Biology* **18**, 1173–1184 (2016).
18. Grumati, P. *et al.* Full length RTN3 regulates turnover of tubular endoplasmic reticulum via selective autophagy. *eLife* **6**, (2017).

19. Smith, M. D. *et al.* CCPG1 Is a Non-canonical Autophagy Cargo Receptor Essential for ER-Phagy and Pancreatic ER Proteostasis. *Developmental Cell* **44**, 217-232.e11 (2018).
20. Chen, Q. *et al.* ATL3 Is a Tubular ER-Phagy Receptor for GABARAP-Mediated Selective Autophagy. *Current Biology* (2019) doi:10.1016/j.cub.2019.01.041.
21. An, H. *et al.* TEX264 Is an Endoplasmic Reticulum-Resident ATG8-Interacting Protein Critical for ER Remodeling during Nutrient Stress. *Molecular Cell* S1097276519302588 (2019) doi:10.1016/j.molcel.2019.03.034.
22. Chino, H., Hatta, T., Natsume, T. & Mizushima, N. Intrinsically Disordered Protein TEX264 Mediates ER-phagy. *Molecular Cell* S1097276519302576 (2019) doi:10.1016/j.molcel.2019.03.033.
23. Yang, H. *et al.* Sequestosome 1/p62 Protein Is Associated with Autophagic Removal of Excess Hepatic Endoplasmic Reticulum in Mice*. *Journal of Biological Chemistry* **291**, 18663–18674 (2016).
24. Nthiga, T. M. *et al.* CALCOCO1 acts with VAMP-associated proteins to mediate ER-phagy. *The EMBO Journal* (2020) doi:10.15252/embj.2019103649.
25. Stephani, M. *et al.* A cross-kingdom conserved ER-phagy receptor maintains endoplasmic reticulum homeostasis during stress. *eLife* **9**, e58396 (2020).
26. Zhao, D. *et al.* A UPR-Induced Soluble ER-Phagy Receptor Acts with VAPs to Confer ER Stress Resistance. *Molecular Cell* **79**, 963-977.e3 (2020).
27. Bhaskara, R. M. *et al.* Curvature induction and membrane remodeling by FAM134B reticulon homology domain assist selective ER-phagy. *Nature Communications* **10**, 2370 (2019).
28. Jiang, X. *et al.* FAM134B oligomerization drives endoplasmic reticulum membrane scission for ER-phagy. *EMBO J* **39**, (2020).
29. Mochida, K. *et al.* Super-assembly of ER-phagy receptor Atg40 induces local ER remodeling at contacts with forming autophagosomal membranes. *Nat Commun* **11**, 1–14 (2020).
30. Chen, S. *et al.* Vps13 is required for the packaging of the ER into autophagosomes during ER-phagy. *Proc Natl Acad Sci USA* 202008923 (2020) doi:10.1073/pnas.2008923117.
31. Liang, J. R. *et al.* A Genome-wide ER-phagy Screen Highlights Key Roles of Mitochondrial Metabolism and ER-Resident UFMylation. *Cell* **180**, 1160-1177.e20 (2020).
32. Yorimitsu, T., Nair, U., Yang, Z. & Klionsky, D. J. Endoplasmic Reticulum Stress Triggers Autophagy. *Journal of Biological Chemistry* **281**, 30299–30304 (2006).
33. Schuck, S., Gallagher, C. M. & Walter, P. ER-phagy mediates selective degradation of endoplasmic reticulum independently of the core autophagy machinery. *Journal of Cell Science* **127**, 4078–4088 (2014).
34. Hu, W. *et al.* A large gene family in fission yeast encodes spore killers that subvert Mendel's law. *eLife* **6**, e26057 (2017).

35. Guglielmi, A. A complete overview of REEP1: old and new insights on its role in hereditary spastic paraplegia and neurodegeneration. *Reviews in the Neurosciences* **31**, 351–362 (2020).
36. Park, S. H., Zhu, P.-P., Parker, R. L. & Blackstone, C. Hereditary spastic paraplegia proteins REEP1, spastin, and atlastin-1 coordinate microtubule interactions with the tubular ER network. *J Clin Invest* **120**, 1097–1110 (2010).
37. Kontou, A., Herman, E. K., Field, M. C., Dacks, J. B. & Koumandou, V. L. Evolution of factors shaping the endoplasmic reticulum. *Traffic* **23**, 462–473 (2022).
38. Fan, S., Liu, H. & Li, L. The REEP family of proteins: Molecular targets and role in pathophysiology. *Pharmacological Research* **185**, 106477 (2022).
39. Björk, S., Hurt, C. M., Ho, V. K. & Angelotti, T. REEPs Are Membrane Shaping Adapter Proteins That Modulate Specific G Protein-Coupled Receptor Trafficking by Affecting ER Cargo Capacity. *PLoS ONE* **8**, e76366 (2013).
40. Schlaitz, A.-L., Thompson, J., Wong, C. C. L., Yates, J. R. & Heald, R. REEP3/4 Ensure Endoplasmic Reticulum Clearance from Metaphase Chromatin and Proper Nuclear Envelope Architecture. *Developmental Cell* **26**, 315–323 (2013).
41. Zhao, D. *et al.* Atg20 and Atg24 family proteins promote organelle autophagy in fission yeast. *Journal of Cell Science* jcs.194373 (2016) doi:10.1242/jcs.194373.
42. Sun, L.-L. *et al.* Global Analysis of Fission Yeast Mating Genes Reveals New Autophagy Factors. *PLoS Genet* **9**, e1003715 (2013).
43. Yu, Z.-Q., Liu, X.-M., Zhao, D., Xu, D.-D. & Du, L.-L. Visual detection of binary, ternary and quaternary protein interactions in fission yeast using a Pil1 co-tethering assay. *Journal of Cell Science* **134**, jcs258774 (2021).
44. Jiang, Z. *et al.* Genetically encoded tags for direct synthesis of EM-visible gold nanoparticles in cells. *Nat Methods* **17**, 937–946 (2020).
45. Beer, K. B. *et al.* Degron-tagged reporters probe membrane topology and enable the specific labelling of membrane-wrapped structures. *Nat Commun* **10**, 3490 (2019).
46. Zhang, X.-R. *et al.* An improved auxin-inducible degron system for fission yeast. *G3 Genes|Genomes|Genetics* **12**, jkab393 (2022).
47. Zhang, D., Vjestica, A. & Oliferenko, S. The cortical ER network limits the permissive zone for actomyosin ring assembly. *Curr Biol* **20**, 1029–1034 (2010).
48. Shibata, Y. *et al.* The Reticulon and Dp1/Yop1p Proteins Form Immobile Oligomers in the Tubular Endoplasmic Reticulum. *Journal of Biological Chemistry* **283**, 18892–18904 (2008).
49. Wang, N. *et al.* Mechanism of membrane-curvature generation by ER-tubule shaping proteins. *Nat Commun* **12**, 568 (2021).
50. Brady, J. P., Claridge, J. K., Smith, P. G. & Schnell, J. R. A conserved amphipathic helix is required for membrane tubule formation by Yop1p. *Proc Natl Acad Sci USA* **112**, E639–E648 (2015).
51. Shibata, Y., Hu, J., Kozlov, M. M. & Rapoport, T. A. Mechanisms Shaping the Membranes of Cellular Organelles. *Annu. Rev. Cell Dev. Biol.* **25**, 329–354 (2009).

52. Evans, R. *et al.* Protein complex prediction with AlphaFold-Multimer. 2021.10.04.463034 Preprint at https://doi.org/10.1101/2021.10.04.463034 (2022).
53. Tsirigos, K. D., Peters, C., Shu, N., Käll, L. & Elofsson, A. The TOPCONS web server for consensus prediction of membrane protein topology and signal peptides. *Nucleic Acids Res* **43**, W401-407 (2015).
54. Gautier, R., Douguet, D., Antonny, B. & Drin, G. HELIQUEST: a web server to screen sequences with specific α-helical properties. *Bioinformatics* **24**, 2101–2102 (2008).
55. Wang, H., Zhang, L., Liddington, R. & Fu, H. Mutations in the Hydrophobic Surface of an Amphipathic Groove of 14-3-3ζ Disrupt Its Interaction with Raf-1 Kinase. *Journal of Biological Chemistry* **273**, 16297–16304 (1998).
56. Elazar, M., Liu, P., Rice, C. M. & Glenn, J. S. An N-Terminal Amphipathic Helix in Hepatitis C Virus (HCV) NS4B Mediates Membrane Association, Correct Localization of Replication Complex Proteins, and HCV RNA Replication. *Journal of Virology* **78**, 11393–11400 (2004).
57. Chino, H. *et al.* Phosphorylation by casein kinase 2 enhances the interaction between ER-phagy receptor TEX264 and ATG8 proteins. *EMBO reports* **23**, e54801 (2022).
58. Chen, S., Cui, Y., Parashar, S., Novick, P. J. & Ferro-Novick, S. ER-phagy requires Lnp1, a protein that stabilizes rearrangements of the ER network. *Proceedings of the National Academy of Sciences* **115**, E6237–E6244 (2018).
59. Cui, Y. *et al.* A COPII subunit acts with an autophagy receptor to target endoplasmic reticulum for degradation. *Science* **365**, 53–60 (2019).
60. Liu, D. *et al.* ER-phagy requires the assembly of actin at sites of contact between the cortical ER and endocytic pits. *Proc. Natl. Acad. Sci. U.S.A.* **119**, e2117554119 (2022).
61. Shima, T., Kirisako, H. & Nakatogawa, H. COPII vesicles contribute to autophagosomal membranes. *Journal of Cell Biology* **218**, 1503–1510 (2019).
62. Wang, N., Shibata, Y., Paulo, J. A., Gygi, S. P. & Rapoport, T. A. *Membrane curvature-generating proteins crucial for autophagosome formation*. http://biorxiv.org/lookup/doi/10.1101/2022.10.27.514035 (2022) doi:10.1101/2022.10.27.514035.
63. Forsburg, S. L. & Rhind, N. Basic methods for fission yeast. *Yeast* **23**, 173–183 (2006).
64. Zhang, X.-R., He, J.-B., Wang, Y.-Z. & Du, L.-L. A Cloning-Free Method for CRISPR/Cas9-Mediated Genome Editing in Fission Yeast. *G3 (Bethesda)* **8**, 2067–2077 (2018).
65. Wei, Y., Wang, H.-T., Zhai, Y., Russell, P. & Du, L.-L. Mdb1, a Fission Yeast Homolog of Human MDC1, Modulates DNA Damage Response and Mitotic Spindle Function. *PLoS ONE* **9**, e97028 (2014).

66. Vještica, A. *et al.* A toolbox of Stable Integration Vectors (SIV) in the fission yeast *Schizosaccharomyces pombe*. *Journal of Cell Science* jcs.240754 (2019) doi:10.1242/jcs.240754.
67. Yu, Z.-Q. *et al.* Atg38-Atg8 interaction in fission yeast establishes a positive feedback loop to promote autophagy. *Autophagy* **16**, 2036–2051 (2020).
68. Hu, W., Suo, F. & Du, L.-L. Bulk Segregant Analysis Reveals the Genetic Basis of a Natural Trait Variation in Fission Yeast. *Genome Biol Evol* **7**, 3496–3510 (2015).
69. Kaiser, C. A. & Schekman, R. Distinct sets of SEC genes govern transport vesicle formation and fusion early in the secretory pathway. *Cell* **61**, 723–733 (1990).
70. Xie, Z., Nair, U. & Klionsky, D. J. Atg8 Controls Phagophore Expansion during Autophagosome Formation. *MBoC* **19**, 3290–3298 (2008).
71. Wouters, E., Vasudevan, L., Crans, R. A. J., Saini, D. K. & Stove, C. P. Luminescence- and Fluorescence-Based Complementation Assays to Screen for GPCR Oligomerization: Current State of the Art. *International Journal of Molecular Sciences* **20**, 2958 (2019).
72. Katoh, K., Rozewicki, J. & Yamada, K. D. MAFFT online service: multiple sequence alignment, interactive sequence choice and visualization. *Briefings in Bioinformatics* **20**, 1160–1166 (2019).
73. Minh, B. Q. *et al.* IQ-TREE 2: New Models and Efficient Methods for Phylogenetic Inference in the Genomic Era. *Molecular Biology and Evolution* **37**, 1530–1534 (2020).
74. Genome-scale phylogeny and contrasting modes of genome evolution in the fungal phylum Ascomycota. *SCIENCE ADVANCES* (2020).

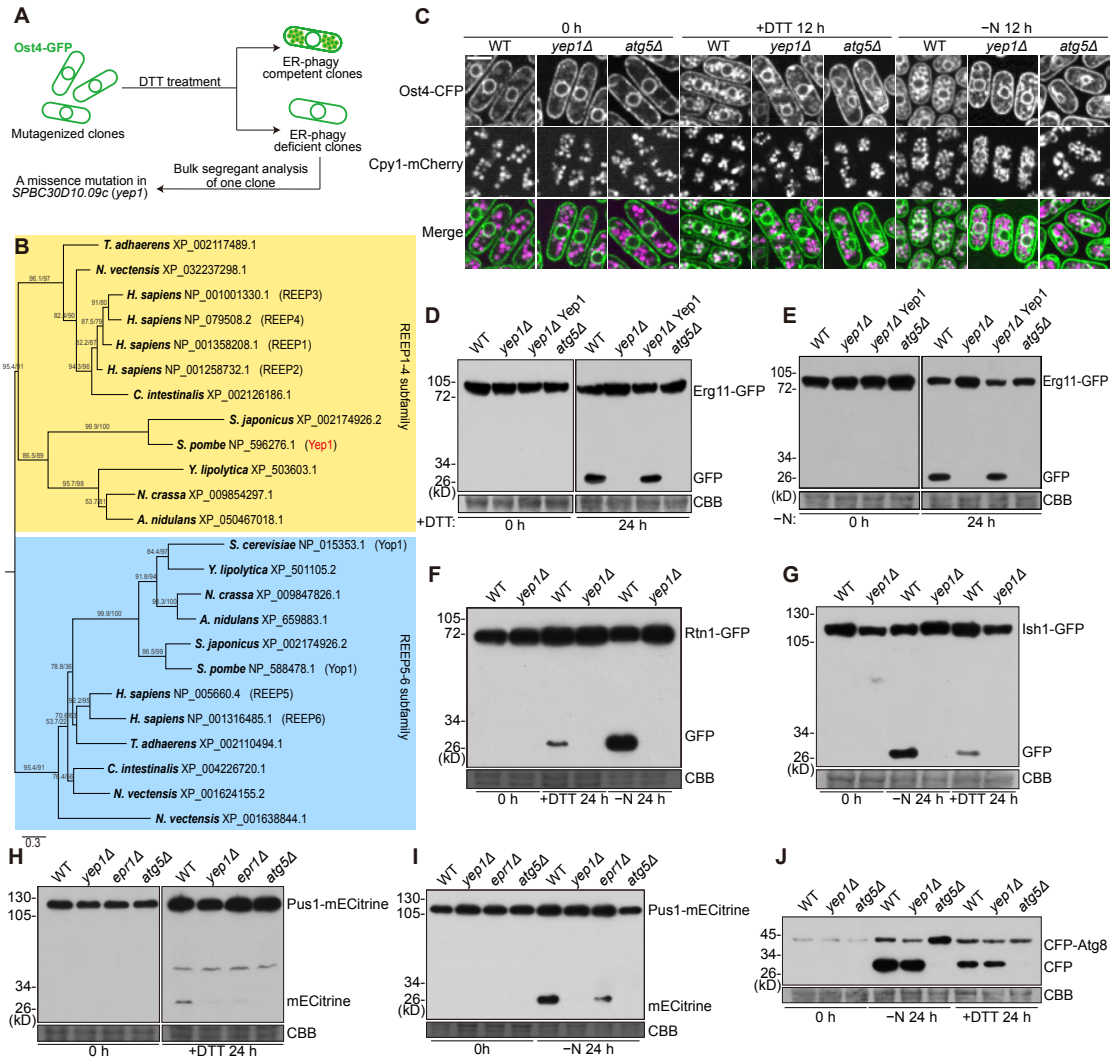

Figure 1. Yep1 is required for ER-phagy and nucleophagy.

(A) Schematic of the imaging-based screen for ER-phagy mutants. Mutagenized clones harboring the Ost4-GFP reporter were treated with DTT for 16 h to induce ER-phagy. The phenotype-causing mutation in an ER-phagy deficient clone was identified by bulk segregant analysis.

(B) Phylogenetic relationships of REEP family proteins in representative metazoan and fungal species. A maximum likelihood tree was constructed using IQ-TREE and rooted by midpoint rooting. Branch labels are the SH-aLRT support values (%) and the UFBoot support values (%) calculated by IQ-TREE. Scale bar indicates 0.3 substitutions per site.

(C) Re-localization of the integral ER membrane protein Ost4-CFP to the vacuole after nitrogen starvation (−N) or DTT treatment (+DTT) was abolished in *yep1Δ* cells.

Wild-type (WT), *yep1Δ*, and *atg5Δ* cells expressing Ost4-CFP were examined by microscopy before and after 12 h starvation or DTT treatment. Cpy1-mCherry is a vacuole lumen marker. Bar, 5 μm.

(D–E) Autophagic processing of the ER membrane protein Erg11-GFP was abolished in *yep1Δ* cells. Cells expressing Erg11-GFP were collected before and after 24 h starvation **(D)** and DTT treatment **(E)**, and total lysates were analyzed by immunoblotting using an antibody against GFP. Post-immunoblotting staining of the PVDF membrane using Coomassie Brilliant Blue (CBB) served as the loading control. The third sample (*yep1Δ* Yep1) is a *yep1Δ* strain transformed with an integrating plasmid expressing Yep1 tagged with mCherry.

(F) Autophagic processing of the cortical ER protein Rtn1-GFP was abolished in *yep1Δ* cells.

(G) Autophagic processing of the nuclear envelope protein Ish1-GFP was abolished in *yep1Δ* cells.

(H) DTT-induced autophagic processing of the nucleoplasmic protein Pus1-mECtrine was abolished in *epr1Δ* and *yep1Δ* cells.

(I) Nitrogen starvation-induced autophagic processing of the nucleus protein Pus1-mECtrine was diminished in *epr1Δ* cells and abolished in *yep1Δ* cells.

(J) Autophagic processing of CFP-Atg8 was largely normal in *yep1Δ* cells.

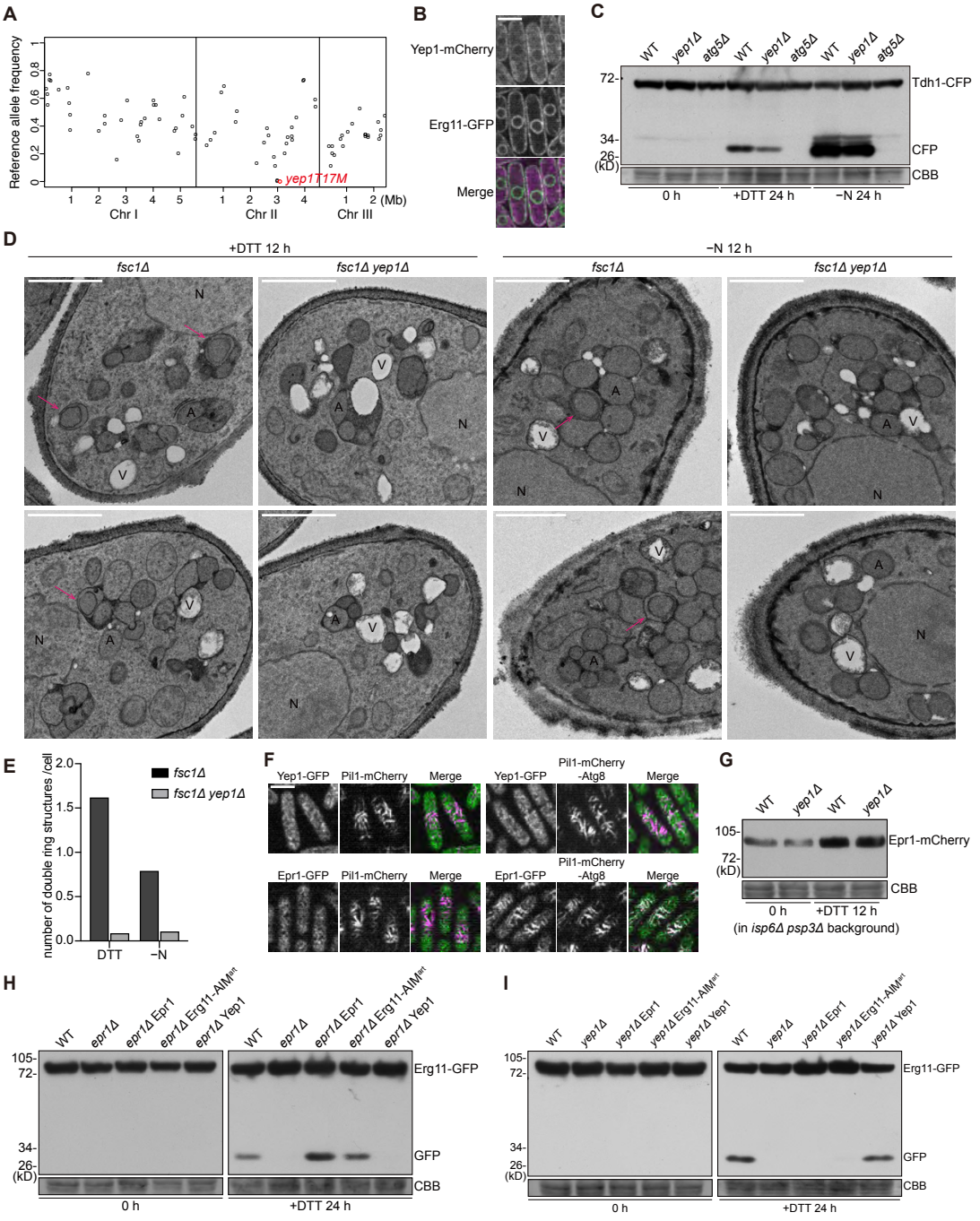

Figure S1. The identification and initial characterization of Yep1 as a factor required for ER-phagy and nucleophagy.

(A) Bulk segregant analysis identifying a mutation in *SPBC30D10.09c* (*yep1*) as a candidate phenotype-causing mutation in an ER-phagy defective mutant. The scatter plot depicts the reference allele frequencies at SNP sites in the pool of the ER-phagy defective segregants derived from a cross between the mutant strain and a wild-type strain. The T17M mutation in *SPBC30D10.09c* (*yep1*) is highlighted in red.

(B) Subcellular localization of Yep1-mCherry expressed from the *P41nmt1* promoter. Log-phase cells co-expressing Yep1-mCherry and the ER marker Erg11-GFP were examined by fluorescence microscopy. Bar, 5 μm.

(C) Autophagic processing of the bulk autophagy marker Tdh1-CFP was largely normal in *yep1Δ* cells.

(D) Electron microscopy analysis of starved and DTT-treated *fsc1Δ* and *fsc1Δ yep1Δ* cells. N, nucleus; V, vacuole; A, autophagosome. Double-ring structures are denoted by pink arrows. Bar, 1 μm.

(E) Quantification of the number of double-ring structures per cell in the analysis shown in (D) (more than 50 cells with autophagosomes were examined for each sample).

(F) Yep1 did not interact with Atg8 in the Pil1 co-tether assay. Log-phase cells co-expressing the bait (Pil1-mCherry or Pil1-mCherry-Atg8) and the prey Yep1-GFP were examined by fluorescence microscopy. Cells co-expressing Pil1-mCherry-Atg8 and Epr1-GFP served as a positive control. Peripheral planes of the cells were imaged. Bar, 5 μm.

(G) Yep1 is not required for the DTT-induced increase of the protein level of Epr1. *isp6Δ psp3Δ* background, which lacks vacuolar protease activities, was used to prevent the degradation of Epr1. Endogenously tagged Epr1-mCherry was analyzed by immunoblotting.

(H) Ectopic expression of Erg11-AIM^{art} but not Yep1 from the *P41nmt1* promoter suppressed the ER-phagy defect of *epr1Δ*.

(I) Ectopic expression of Erg11-AIM^{art} or Epr1 did not rescue the ER-phagy defect of *yep1Δ*.

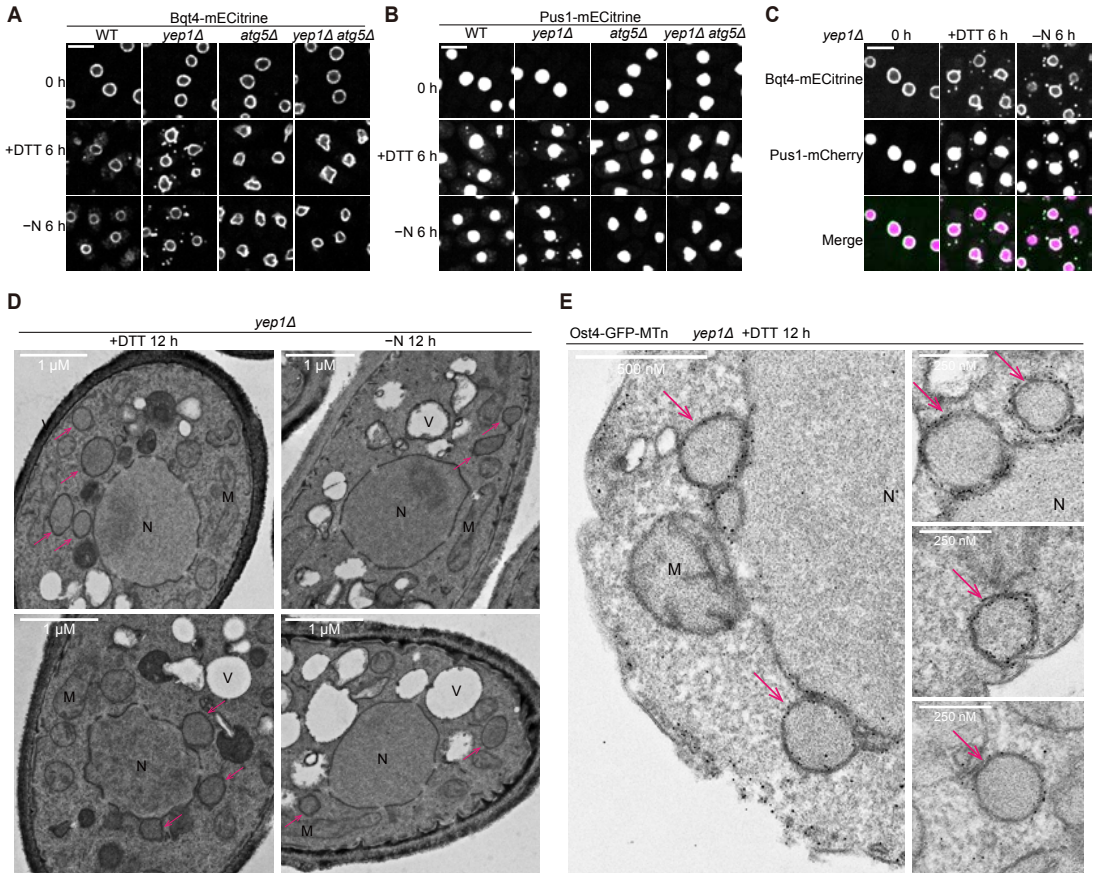

Figure 2. Yep1 is required for the autophagosomal enclosure of ER-phagy and nucleophagy cargos.

(A) Bqt4-mECtrine formed cytoplasmic puncta in *yep1Δ* cells after nitrogen starvation or DTT treatment. Bar, 5 μm.

(B) Pus1-mECtrine formed cytoplasmic puncta in *yep1Δ* cells after nitrogen starvation or DTT treatment. Bar, 5 μm.

(C) The co-localization between Bqt4 puncta and Pus1 puncta accumulated in *yep1Δ* cells. Bar, 5 μm.

(D) Electron microscopy analysis of *yep1Δ* cells treated with DTT or nitrogen starvation. N, nucleus; V, vacuole; M, mitochondrion. Ring-shaped membrane structures are denoted by pink arrows. Bar, 1 μm.

(E) Electron microscopy analysis of gold nanoparticle-labeled membrane structures of the ER/nuclear envelope origin in *yep1Δ* cells. MTn tagging of Ost4 allowed membrane structures of the ER/nuclear envelope origin to be labeled by EM-visible gold

nanoparticles. N, nucleus; M, mitochondrion. Gold nanoparticle-labeled ring-shaped membrane structures are denoted by pink arrows.

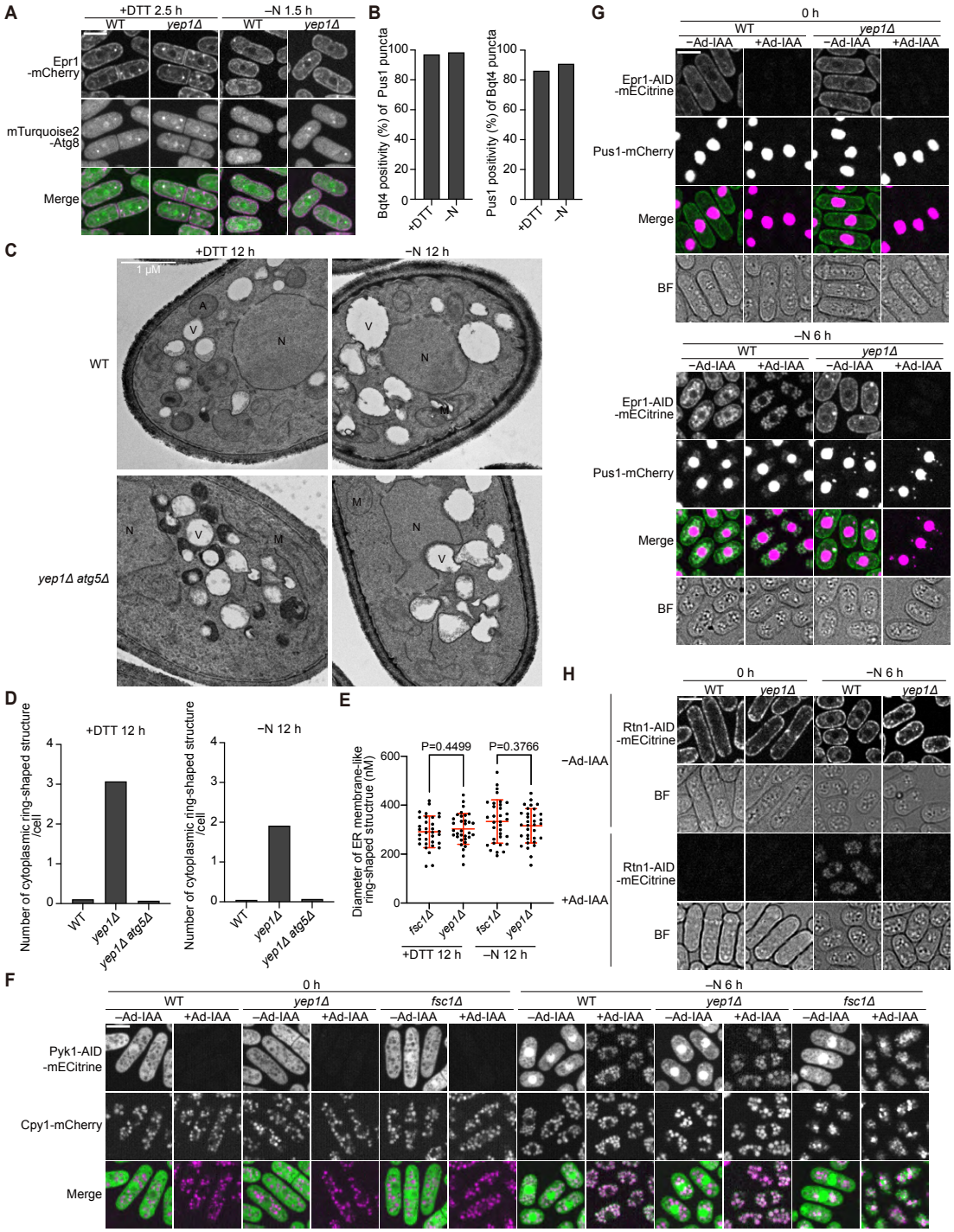

Figure S2. Yep1 is required for the autophagosomal enclosure of ER-phagy and nucleophagy cargos.

(A) Yep1 is not required for the co-localization of Epr1 and Atg8 at punctate structures shortly after ER-phagy induction. Wild-type and *yep1Δ* cells co-expressing Epr1-mCherry and mTurquoise2-Atg8 were examined by microscopy after 2.5 h DTT or 1.5 h starvation treatment. Bar, 5 μm.

(B) Quantification of the co-localization between Bqt4 puncta and Pus1 puncta in the analysis shown in Figure 2C (more than 250 puncta were examined for each sample).

(C) Electron microscopy analysis of nitrogen-starved and DTT-treated wild-type and *yep1Δ atg5Δ* cells. N, nucleus; V, vacuole; M, mitochondrion; A, autophagosome. Bar, 1 μm.

(D) Quantification of the number of cytoplasmic ring-shaped structures in the analysis shown in Figure 2D and Figure S2C (more than 30 cells were examined for each sample). Autophagosomes, which are ring-shaped structures juxtaposed to vacuoles, were excluded from this quantification.

(E) Quantification of the diameters of the ring-shaped structures in *yep1Δ* cells in the analysis shown in Figure 2C and the inner rings in the double-ring structures in the *fsc1Δ* cells in the analysis shown in Figure S1D. P-values were calculated using Welch's t-test.

(F) Applying the degron protection assay on the cytosolic protein Pyk1-AID-mECitrine. Prior to observation, cells were treated with (+Ad-IAA) or without (−Ad-IAA) 5-adamantyl-IAA for 1.5 h. BF, brightfield. Cpy1-mCherry is a vacuole lumen marker. Bar, 5 μm.

(G) Applying the degron protection assay on Epr1-AID-mECitrine. BF, brightfield. Bar, 5 μm.

(H) Applying the degron protection assay on Rtn1-AID-mECitrine. BF, brightfield. Bar, 5 μm.

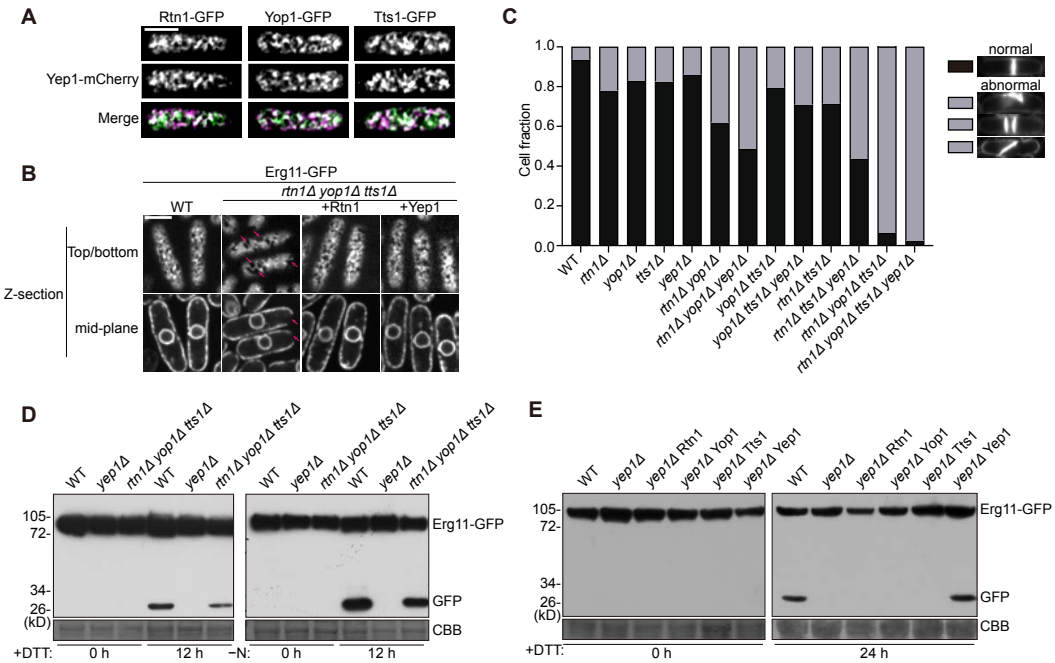

Figure 3. Yep1 possesses the ability to shape the ER membrane.

(A) Yep1 co-localized with ER-shaping proteins. Single optical sections focused on the top (or bottom) of the cells are shown. Images were processed by deconvolution to allow better visualization of the cortical ER network. Bar, 5 μm.

(B) The aberrant cortical ER morphology of *rtn1Δ yop1Δ tts1Δ* cells can be partially rescued by the overexpression of Yep1. A peripheral plane and a central plane of the same cells are shown. Red arrows denote the large holes in images of the peripheral planes or the extended gaps in images of the central planes. Images were processed by deconvolution to allow better visualization of the cortical ER network. Bar, 5 μm.

(C) Quantification of the septum abnormality phenotypes (more than 200 cells with septa were examined for each sample). The septum abnormality phenotypes include long-axis septum, multiple septa, and tilted septum. Septa were visualized by calcofluor staining.

(D) ER-phagy induced by DTT treatment or nitrogen starvation was largely normal in the absence of Rtn1, Yop1, and Tts1.

(E) The ER-phagy defect of *yep1Δ* cells was not suppressed by the ectopic expression of Rtn1, Yop1, or Tts1.

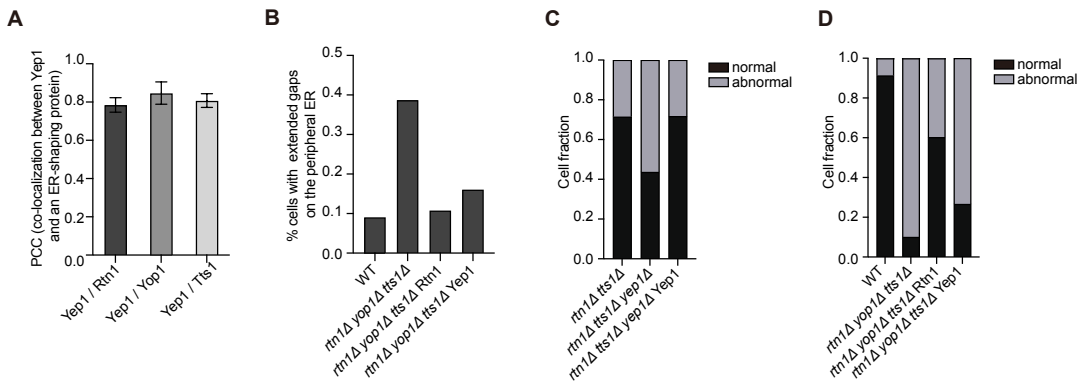

Figure S3. Yep1 possesses the ability to shape the ER membrane.

(A) Co-localization between Yep1-mCherry and Rtn1-GFP, Yop1-GFP, or Tts1-GFP was quantitated using Pearson's correlation coefficient (PCC). The PCC values are presented as mean±s.d. (n=10 cells).

(B) Quantification of the percentages of cells with extended gaps in images of the mid-plane in the analysis shown in Figure 3B (more than 300 cells were examined for each sample).

(C–D) Quantification of the septum abnormality phenotypes (more than 200 cells with septa were examined for each sample).

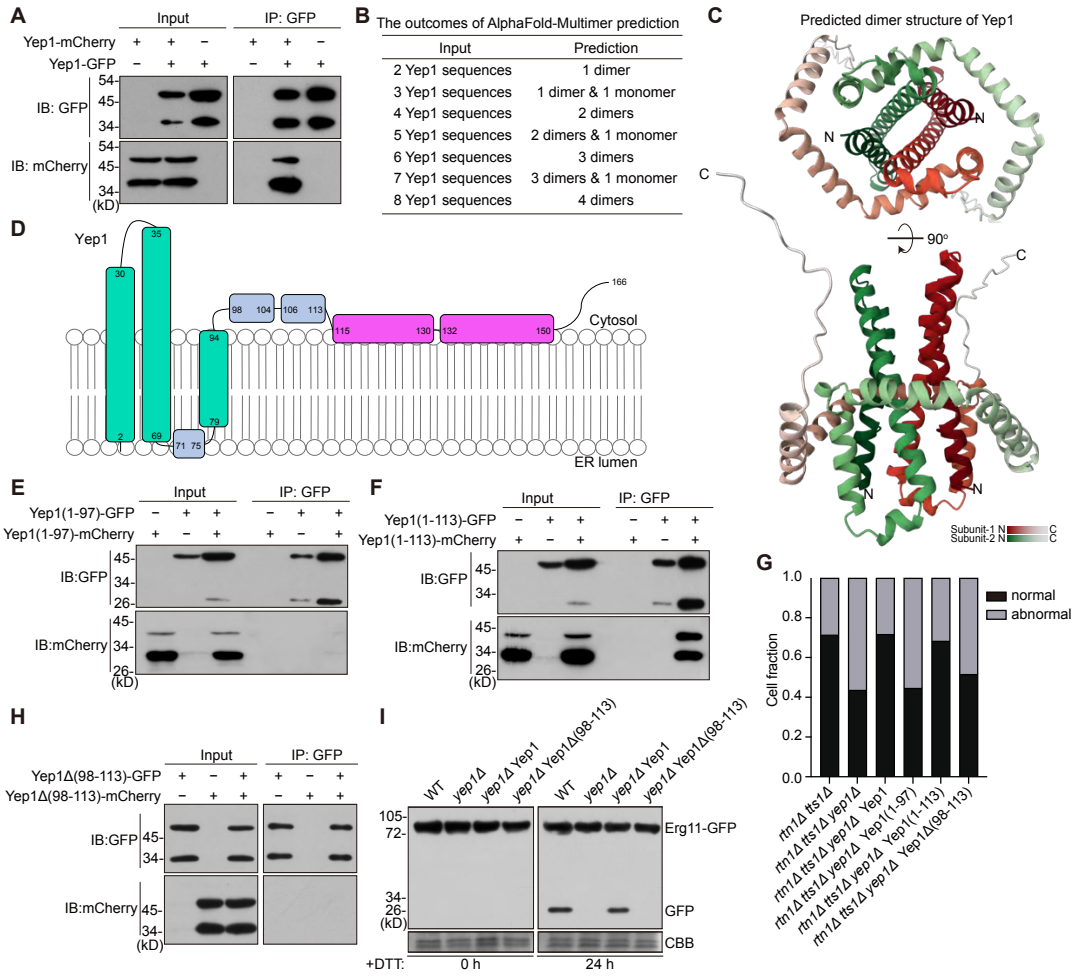

Figure 4. Yep1 self-interaction is important for its membrane-shaping ability and ER-phagy function.

(A) Yep1 exhibited self-interaction. Yep1-GFP was immunoprecipitated and co-immunoprecipitation of Yep1-mCherry was analyzed by immunoblotting.

(B) The outcomes of predicting the structures of Yep1 oligomers using AlphaFold-Multimer.

(C) The AlphaFold-Multimer-predicted Yep1 homo-dimer structure shown in the cartoon representation. Each subunit is shown by a color gradient from the N-terminus (red or green) to the C-terminus (silver).

(D) Topology model of Yep1. The secondary structure is based on the predicted 3D structure shown in (C). The topology is based on the TOPCONS membrane protein topology prediction shown in Figure S4C. Transmembrane helices (TMHs) are colored

green. The two C-terminal amphipathic helices (APHs) are colored magenta (see Figure 5C). Other α-helices are colored light blue.

(E) Yep1(1-97) did not exhibit self-interaction in a co-immunoprecipitation analysis.

(F) Yep1(1-113) exhibited self-interaction in a co-immunoprecipitation analysis.

(G) Quantification of the septum abnormality phenotypes of *rtn1Δ tts1Δ* cells, *rtn1Δ tts1Δ yep1Δ* cells, and *rtn1Δ tts1Δ yep1Δ* cells expressing full-length Yep1, Yep1(1-97), Yep1(1-113), or Yep1Δ(98-113) (more than 200 cells with septa were examined for each sample).

(H) Yep1Δ(98-113) did not exhibit self-interaction in a co-immunoprecipitation analysis.

(I) Yep1Δ(98-113) was unable to rescue the ER-phagy defect of *yep1Δ*.

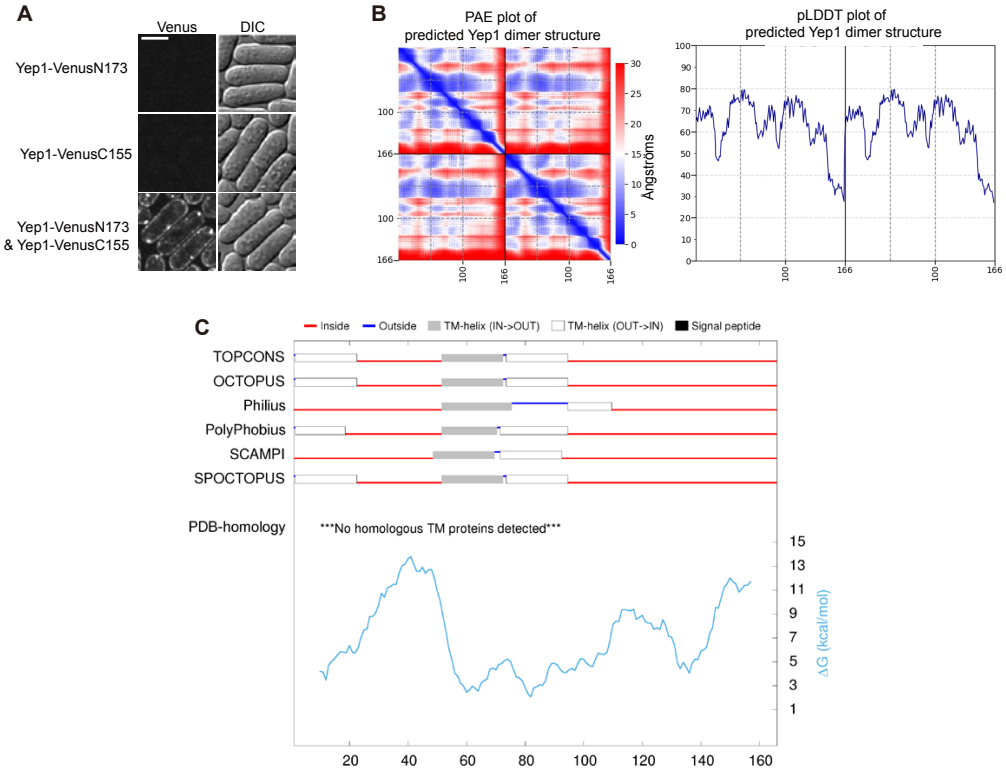

Figure S4. Yep1 self-interaction, the predicted structure of the Yep1 dimer, and the predicted topology of Yep1.

(A) Yep1 exhibited self-interaction in the BiFC assay. Log-phase cells expressing Yep1-VenusN173 alone, Yep1-VenusC155 alone, or both were examined by fluorescence microscopy. Bar, 5 µm.

(B) The predicted aligned error (PAE) plot and pLDDT plot of the AlphaFold-Multimer-predicted structure of the Yep1 homo-dimer shown in Figure 4C.

(C) TOPCONS membrane protein topology prediction for Yep1.

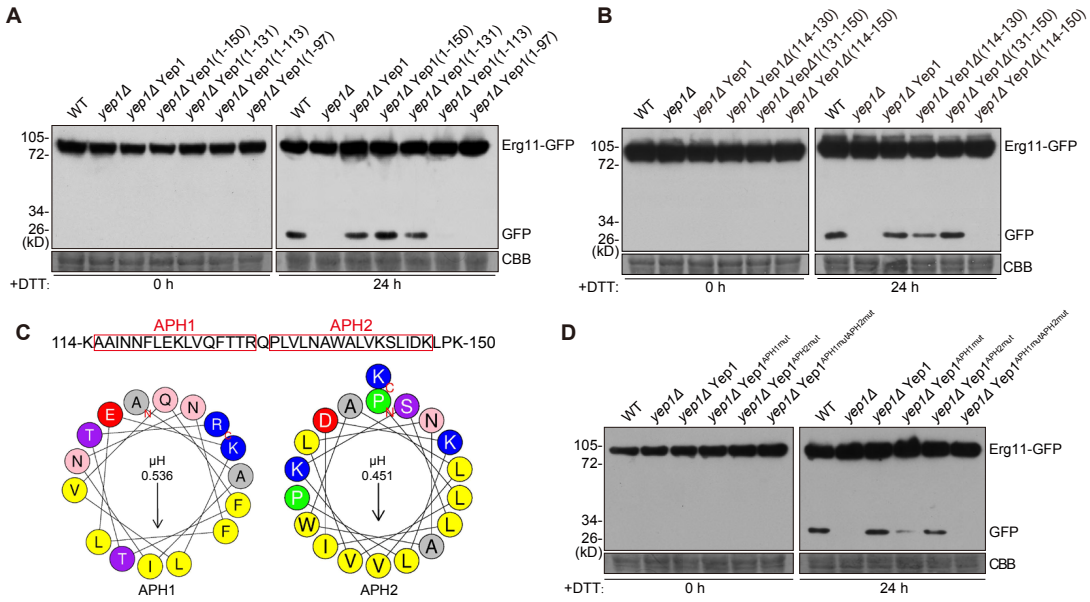

Figure 5. APHs of Yep1 are essential for its ER-phagy function.

(A) Yep1(1-131) or Yep1(1-150), but not Yep1(1-113), is able to support ER-phagy.

(B) Internal deletion of both but not either one of the two APHs abolished the ER-phagy function of Yep1.

(C) Helical wheel representations of two APHs of Yep1. The helical wheels were generated using HeliQuest. Hydrophobic residues are colored in yellow, hydrophilic residues in blue (R and K), red (D and E), purple (T and S), and pink (N and Q), alanine in grey, and proline in green. The HeliQuest-calculated hydrophobic moment (μH) of the helix is shown.

(D) The amphipathic nature of APHs is important for the ER-phagy function of Yep1. Yep1^{APH1mut} harbors the I117D, F120D, and L124D mutations; Yep1^{APH2mut} harbors the A137D, V141D, and L148D mutations; Yep1^{APH1mutAPH2mut} harbors the I117D, F120D, L124D, A137D, V141D, and L148D mutations (see helical wheel representations in Figure S5G).

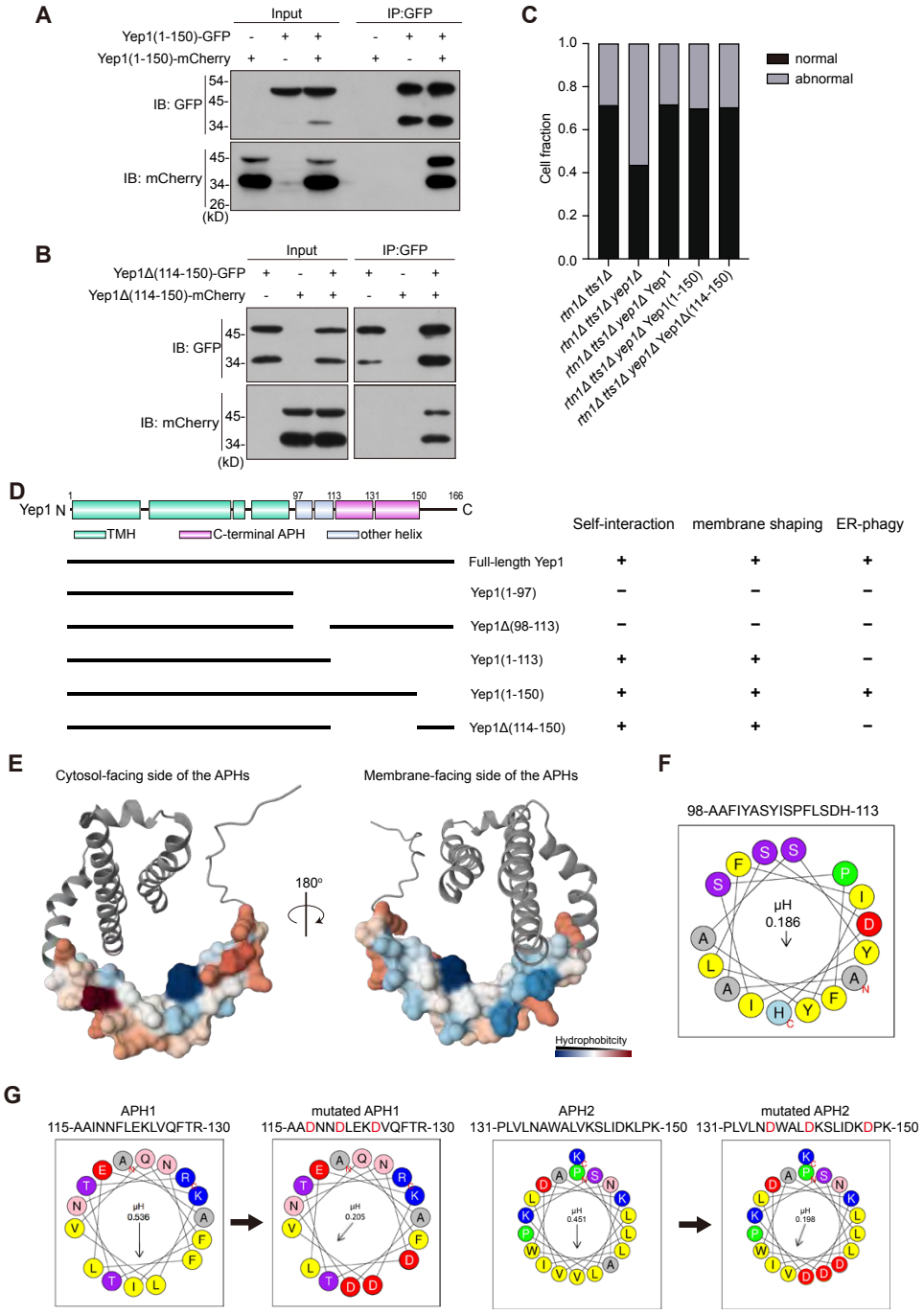

Figure S5. APHs of Yep1 are essential for its ER-phagy function.

(A) Yep1(1-150) exhibited self-interaction in a co-immunoprecipitation analysis.

(B) Yep1Δ(114-150) exhibited self-interaction in a co-immunoprecipitation analysis.

(C) Quantification of the septum abnormality phenotypes in *rtn1Δ tts1Δ* cells, *rtn1Δ tts1Δ yep1Δ* cells, and *rtn1Δ tts1Δ yep1Δ* cells expressing full-length Yep1, Yep1(1-150), or Yep1Δ(114-150) (more than 200 cells with septa were examined for each sample).

(D) Summary of the truncation and internal deletion analysis of Yep1.

(E) The amphipathic nature of APHs is visualized in the AlphaFold-Multimer-predicted structure. The two APHs and the intervening amino acid are shown in the surface representation and are colored base on hydrophobicity. The rest of Yep1 is shown in the cartoon representation.

(F) Helical wheel representation and the hydrophobic moment (μH) of residues 97-113 of Yep1.

(G) Helical wheel representations and the hydrophobic moments (μH) of APHs and mutated APHs.

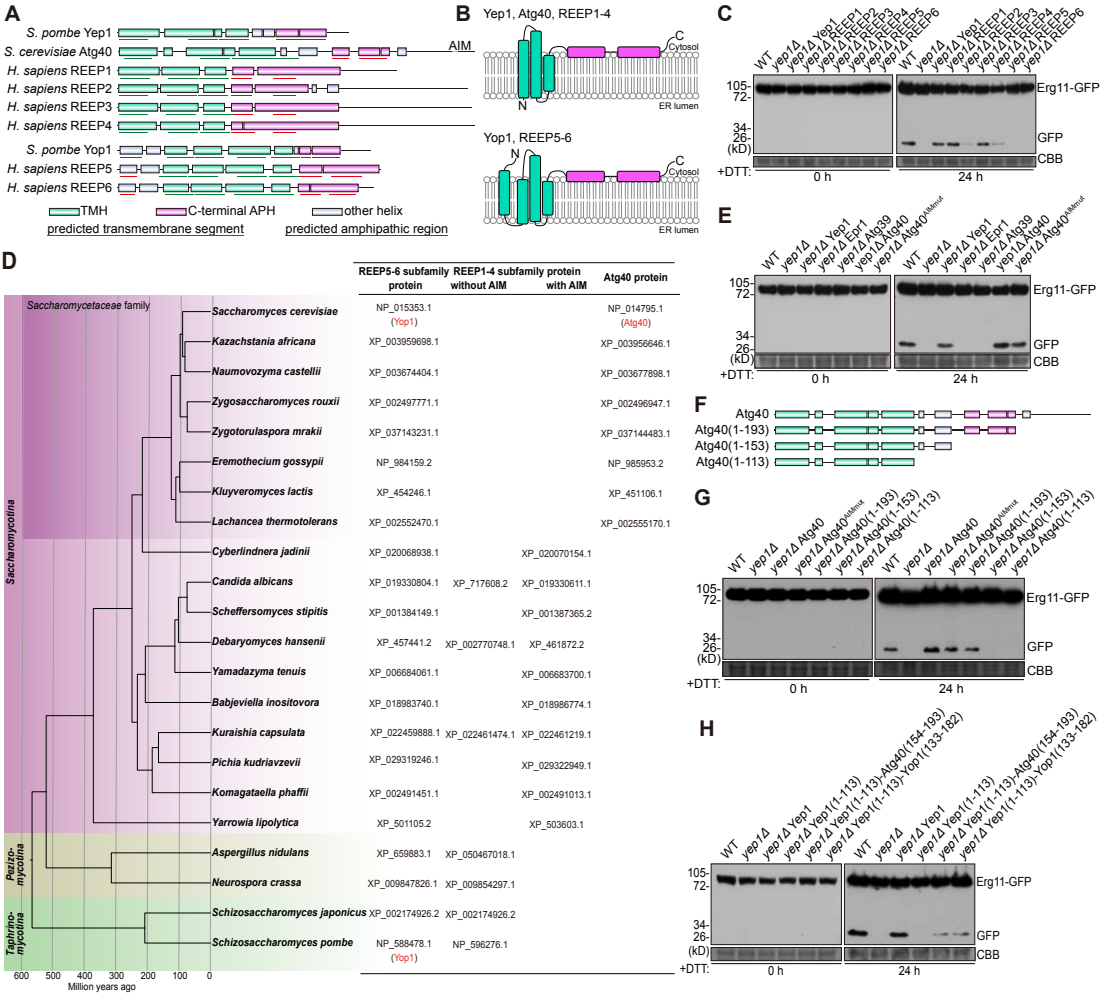

Figure 6. REEP1-4 subfamily proteins and Atg40 share the same ER-phagy function with Yep1.

(A) Schematics of predicted structures of representative members of the REEP family and *S. cerevisiae* Atg40. The depicted structural elements are based on AlphaFold predicted structures, TOPCONS prediction of membrane topology, and HeliQuest analysis of APHs.

(B) Topology models of representative REEP family ptoteins and Atg40. Transmembrane helices (TMHs) are colored green. C-terminal APHs are colored magenta.

(C) The ER-phagy defect of *yep1Δ* can be suppressed by expressing any one of the four human REEP1-4 subfamily proteins but not by expressing human REEP5 or REEP6.

(D) *S. cerevisiae* Atg40 and its PSI-BLAST-detectable sequence homologs in other *Saccharomycetaceae* species (referred to as Atg40 proteins here) are likely divergent REEP1-4 subfamily proteins. Shown on the left is a time-calibrated species tree of representative *Ascomycota* species[74]. REEP5-6 subfamily proteins, REEP1-4 subfamily proteins, and Atg40 proteins present in these species are listed on the right. All Atg40 proteins and some REEP1-4 subfamily proteins harbor a C-terminal AIM (see Figure S7C).

(E) Expressing *S. cerevisiae* Atg40 rescued the ER-phagy defect of *yep1Δ* in a manner independent of its Atg8-interacting motif (AIM). $Atg40^{AIMmut}$ harbors the Y242A and M245A mutations.

(F) Schematics of wild-type and truncated Atg40.

(G) Atg40(1-193) but not Atg40(1-153) rescued the ER-phagy defect of *yep1Δ*.

(H) Fusing an APH-containing fragment from either *S. cerevisiae* Atg40 or *S. pombe* Yop1 to Yep1(1-113) can partially restore its ER-phagy function.

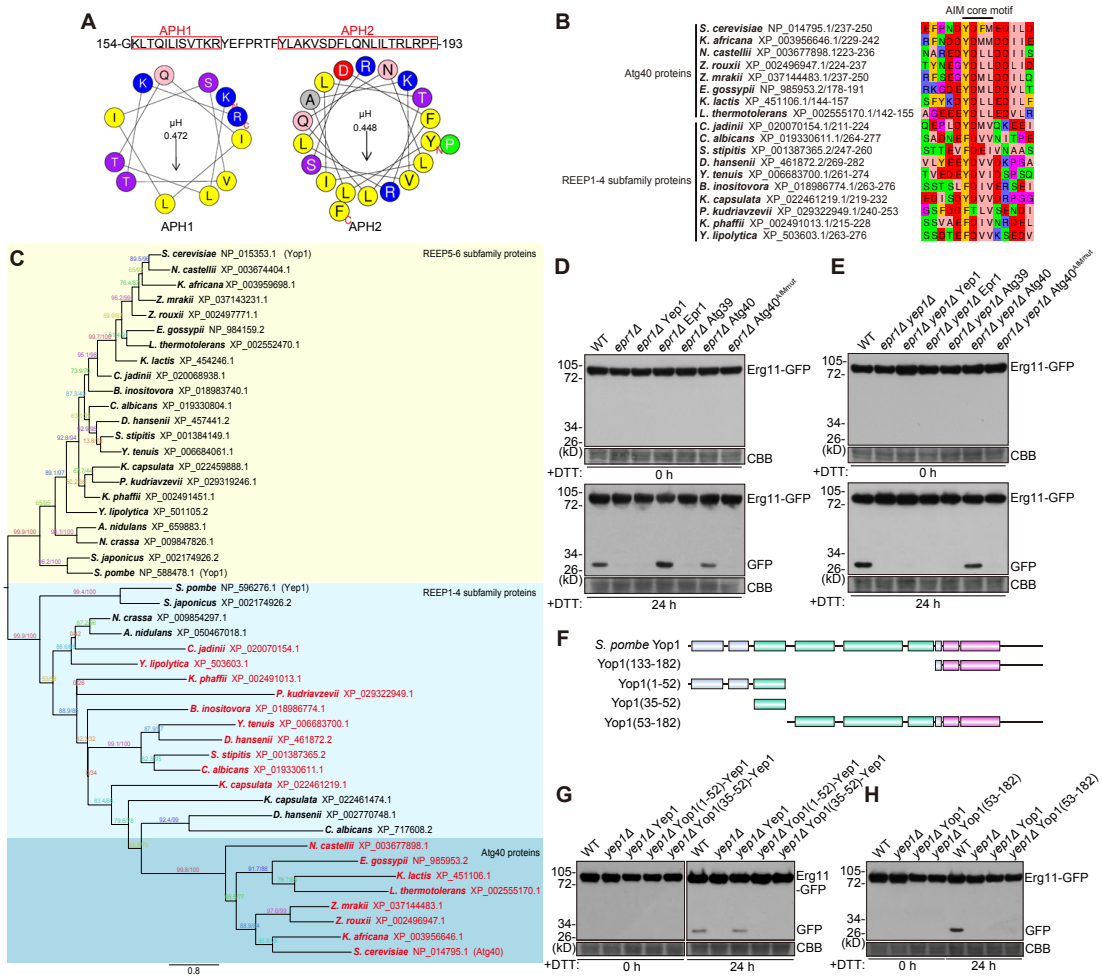

Figure S6. REEP1-4 subfamily proteins and Atg40 share the same ER-phagy function with Yep1.

(A) Helical wheel representations and the hydrophobic moments (μH) of the two C-terminal APHs in Atg40.

(B) The alignment of the C-terminal AIM in the proteins whose names are colored red in Figure S6C. The AIM core motif is highlighted.

(C) Phylogenetic relationships of REEP family proteins and Atg40 proteins in representative *Ascomycota* species. The sequences of REEP family proteins were retrieved by PSI-BLAST from the NCBI refseq_protein database using the sequences of *Yarrowia lipolytica* orthologs of *S. pombe* Yop1 and Yep1 as queries. The sequences of Atg40 proteins were retrieved by PSI-BLAST from the NCBI refseq_protein database using the sequence of *S. cerevisiae* Atg40 as query. A sequence alignment was generated using MAFFT and a maximum likelihood tree was constructed using IQ-

TREE. The tree was rooted using the REEP5-6 subfamily proteins as outgroup. Branch labels are the SH-aLRT support values (%) and the UFBoot support values (%) calculated by IQ-TREE. The names of proteins containing a C-terminal AIM are colored red. The scale bar indicates 0.8 substitutions per site.

(E) *S. cerevisiae* Atg40 rescued the ER-phagy defect of *epr1Δ* in a manner dependent on its Atg8-interacting motif (AIM). $Atg40^{AIMmut}$ harbors the Y242A and M245A mutations.

(F) *S. cerevisiae* Atg40 rescued the ER-phagy defect of *epr1Δ yep1Δ* in a manner dependent on its AIM.

(G) Schematics of wild-type and truncated Yop1. Yop1(133-182) appears in Figure 6H. Yop1(1-52) and Yop1(35-52) appear in Figure S6H. Yop1(53-182) appears in Figure S6I.

(H) Adding an extra N-terminal transmembrane helix (TMH) to Yep1 disrupted its ER-phagy function. Yop1(1-52) includes the N-terminal cytosolic region and the first TMH of Yop1. Yop1(35-52) includes only the first TMH of Yop1.

(I) Removing the N-terminal region of Yop1 upstream of its second TMH did not render it capable of substituting for Yep1. Yop1(53-182) lacks the N-terminal cytosolic region and the first TMH.

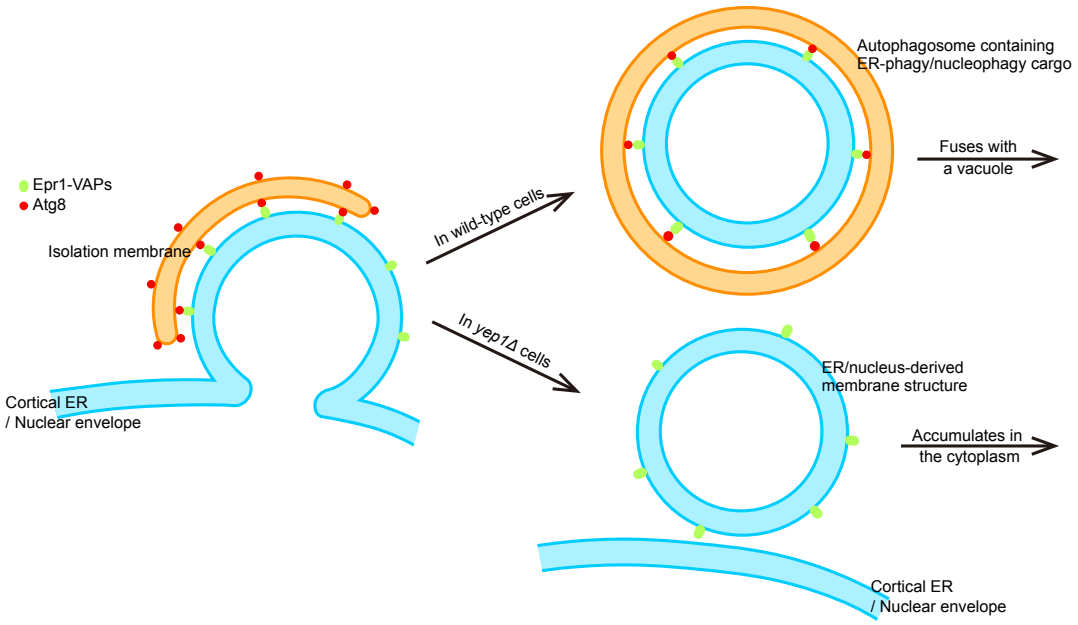

Figure 7. Schematic depicting how ER-phagy/nucleophagy fails in the absence of Yep1.

Yep1 is indispensable for the autophagosomal enclosure of cargos during ER-phagy and nucleophagy. In wild-type cells, ER-phagy/nucleophagy cargos are sequestered into autophagosomes after their separation from the source membrane compartments. In the absence of Yep1, the recruitment of the autophagic machinery at the early phase of ER-phagy/nucleophagy occurs normally, ER-phagy/nucleophagy cargos can separate from the source membrane compartments but fail to be enclosed within autophagosomes, resulting in the accumulation of ER- and nucleus-derived membrane structures in the cytoplasm.